Engineering Science & Technology
http://ojs.wiserpub.com/index.php/EST/

Review

Condition Synthesis and Performance of Alkali-Activated Composites Incorporating Clay-Based Materials-A Review

Rodrigue Cyriaque Kaze

Department of Minerals Engineering, School of Chemical Engineering and Mineral Industries, University of Ngaoundere, Ngaoundere P.O. Box 454, Cameroon
Email: kazerodrigue@gmail.com

Received: 26 January 2024; **Revised:** 11 May 2024; **Accepted:** 22 May 2024

Abstract: Studies over the years have shown that alkali-activated composite (AAC) binders are viable alternatives to conventional Portland cement (PC) composites. However, the increasing interest in AACs for the construction of various infrastructures has created a need to find alternatives to the conventional materials used in their production. Various types of 1:1 clay, which are available in different forms across different parts of the world, can be used as an aluminosilicate source in the production of AACs. However, compared to the use of conventional aluminosilicate sources such as slag and fly ash, there is limited understanding, research, and application of AAC incorporating clay-based materials. Thus, this comprehensive review was carried out to explore and discuss various properties of AACs made with clayey materials. Both the fresh and hardened properties of clay-based AACs are discussed, including the effects of different alkaline solution types, their concentrations, the combination of alkaline activators, the fine aggregate-to-binder ratio, the alkaline solution-to-binder ratio, and the curing temperature and duration. However, in terms of the hardened properties, more focus is placed on durability performance as these properties are critical to the behaviour of the AACs in various environments.

***Keywords*:** alkali-activated composites, clay, sustainability, construction material, geopolymer

1. Introduction

The broadest category, which is known as alkali-activated material (AAM), includes virtually any binder system that is produced through the reaction of a solid aluminosilicate powder with an alkali metal source, whether it be dissolved or solid [1]-[2]. Many times, geopolymers [3] are thought of as a subset of AAMs, with nearly all of the binding phases being highly coordinated aluminosilicate [4]-[5]. Alkali-activated materials and geopolymer are obtained at lower temperatures (less than 100 °C) compared to Portland cement which requires high energy and releases about 5% of CO_2 emissions. Nowadays, the study of geopolymer or alkali-activated materials has gained more attention, since they are considered alternative materials to conventional Portland cement because they are environmentally friendly, with low CO_2 emissions in their production processes.

The use of alkali-activated composites (AACs) for various construction purposes is increasing due to their viability to be used as a sustainable alternative to the conventional Portland cement (PC) composite [6]. In addition, AACs have been found to exhibit higher or similar performance as those of PC composites [7]-[8]. AACs are made

DOI: https://doi.org/10.37256/est.5220244366

with binders composed of an activator (e.g., acidic or alkaline solution) and aluminosilicate precursor(s) at relatively low temperatures (≤ 100 °C). The conventional precursors used in AACs are mostly waste/by-products such as fly ash [9]-[10], slag [11]-[13], rice husk ash [14]-[15], laterite [16], waste fired bricks [17], waste marble [18] volcanic ashes [19]-[20], red mud [21]-[23], and glass powder [8], [24], etc. while the common activators used are sodium silicate and sodium hydroxide [25]-[27]. Other studies elsewhere [28] investigated the effect of glass powder (up to 25%) on the microstructure and durability properties of slag-fly ash-based alkali-activated pavement concrete mixes and found that 15% of glass ensured high performance and good durability. The same authors used glass powder as a binder ingredient for slag-fly ash-based alkali-activated concrete for paver applications [28]. On the other hand, locally available materials with certain chemical properties can also be utilized in the synthesis of AACs. Of such locally available materials that are available in various parts of the world in large quantities are clay soils [29]-[30]. Clay with various chemical compositions can be processed and used as a precursor candidate in the production of AACs. As clay soils are composed of a significant amount of aluminate and silicate they can be used as an aluminosilicate source in the synthesis of AACs [31].

Predominately, the clay used for AACs can be calcined at various elevated temperatures to increase the reactivity of the clay which would enhance the dissolution of the monomers when an alkali medium is added [11], [32]-[33]. The calcination temperature of clay used in AACs ranges from 500 °C to 900 °C [34]. The reactivity of the clay materials is increased after calcination due to the transformation of the crystalline phases into amorphous phases which are reactive [35]. However, several other studies have also shown that uncalcined clay can also be utilized in the synthesis of AACs. Wang et al. [36] comparatively investigated the appearance change, mass change, and unconfined compressive strength (UCS) of cement and slag-fly ash-based geopolymer-stabilized soil under Na_2SO_4 erosion. After investigation, they realized that the sulfate resistance of stabilized soil was significantly affected by the stabilizer type. They concluded that the cement-stabilized soil significantly deteriorated with erosion age due to expansion caused by the calcium Aluminate Ferrite trisubstituted (Aft) when subjected to a sulfate environment compared to geopolymer stabilized soils treated in the same medium. A similar study was conducted by Su et al. [37] where the authors focused on the feasibility and performance improvement of sustainable slag/fly ash-based geopolymer in the solidification of organic clay. From their study, it has been demonstrated that sustainable geopolymer outperforms cement in enhancing the physical-mechanical characteristics of organic clay. Ayawnna et al. [38] reinforced the mechanical of metakaolin-based geopolymer with glass fiber and bamboo fiber. They found that adding 1%, 3%, and 5% by volume of BF, fiber improved the mechanical properties by 1.9, 2.5, and 2.6 times while glass fiber developed poor matrix with no improvement. Trindade et al. [39] used auxetic fabrics mainly composed of basalt fiber as reinforcement for the geopolymer composites. After investigation, they observed the increased mechanical properties, up to 26 MPa in tension and 12.8 MPa in flexural strength. Zhang et al. [40] modified the metakaolin-based geopolymer matrix with silane and epoxy resin and then investigated its effects and interaction mechanism on mechanical properties. The polymerization between the organic agents and geopolymer gel gives the WR and SCA modified MG composites, as determined by isothermal conductivity calorimetry (ICC) analysis, a higher reaction degree than pure geopolymer justifying the increased performance recorded on modified geopolymer matrix.

Various AACs, such as paste (aluminosilicate precursor with an alkaline activator), mortar (aluminosilicate precursor + sand with an alkaline activator), and concrete (aluminosilicate precursor + sand + aggregates with an alkaline activator), have been produced using clayey materials. Out of the numerous types of clay, the most common ones used in AACs are kaolinite and metakaolin. Metakaolin is obtained after the kaolinite has undergone calcination. As shown in Figure 1, both kaolinite and metakaolin have a dioctahedral layered structure. However, the layered structure of metakaolin is more open compared to that of kaolinite. As shown in Figure 1, the structure of kaolin and calcined kaolin is plate-like. The particles formed a structure resembling layers, appearing as plates [41]. Kaolin undergoes dehydroxylation during calcination, but its plate-like structure remains unaltered [42]. The process of converting kaolin into calcined kaolin can be easily observed through the use of infrared spectroscopy.

Compared to the conventional precursors used in the synthesis of AACs, there are numerous research reports on the development of AACs from clay. Thus, create more awareness about the potential use of clay-based AACs, this comprehensive review was carried out to explore and discuss the properties of various clay-based AACs. The properties of clay-based AACs explored in this review paper are durability properties, mechanical and microstructural properties, and fresh properties. More emphasis was placed on the durability properties as these properties are very

critical to the long-term performance of AACs and also provide an insight into how the composites would perform in various environments. It is anticipated that the discussions made in this paper will gear more research, development, and application of clay-based AACs in the construction of various infrastructures. The purpose of this paper is to provide an update on the research on AACs made from fly ash, volcanic ash, and blast furnace slag-the three main aluminosilicate materials. Additionally, this paper serves as a reference for future research aimed at producing an alkali-activated material based on fly ash, volcanic ash, and blast furnace slag that has the necessary mechanical properties and durability through appropriate mix design and additive use. The objective of this review article is to study the fresh and hardened properties, durability, and effect of various calcined clay additives (raw kaolinitic clay, metakaolin, and meta-halloysite) and non-clay additives (pegmatite, granite, quartz sand, and felspar) in AAC-mortar or binders. The mechanical properties were evaluated in terms of different physical and chemical parameters, such as the type of alkali activator, the concentration of sodium hydroxide solution, the solution to binder ratio, sodium silicate to sodium hydroxide ratio, curing regime, etc. which makes the design complicated than OPC mortar or paste. The research results of each property are reviewed, compared, and analysed to provide a reference for future research on AACs (binders, mortars, and concretes).

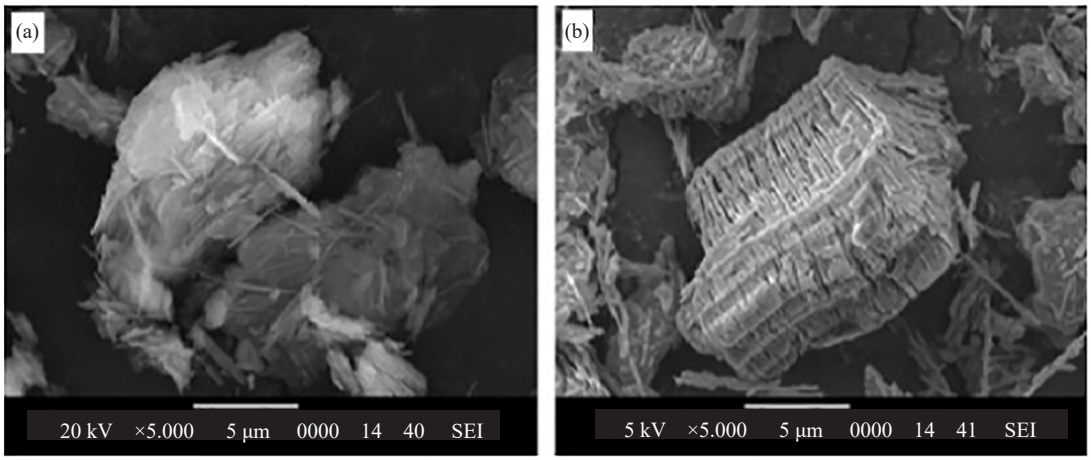

Figure 1. Clay materials in AACs (a) kaolinite and (b) metakaolin [43]

2. AACs incorporating clay-based materials

2.1 *Fresh properties*

2.1.1 *Workability*

The workability of alkali-activated binders is greatly influenced by the activator solutions used, the liquid-to-solid ratio, their concentration, and additives. Duan et al. [44] investigated the addition of metakaolin up to 25 wt% (as secondary source material) on the workability of fly ash-based AAC. Findings from the study indicated that as the metakaolin content increased, the flow diameter of fresh ACC samples decreased. This decrease in flow with the incorporation of metakaolin was linked to the high specific surface of metakaolin which resulted in high demand for mixing water. Similarly, Alanazi et al. [45] investigated the effects of some mineral additives (i.e., slag, silica fume, and metakaolin) on the workability of fly ash-based AAC, and the results compared with that of PC composites. Results from the study showed that the use of mineral additives such as metakaolin and silica fume resulted in a decrease in the flow values. The decrease in flow values when incorporating silica fume and metakaolin was ascribed to the high specific surface area and the finer particles of the additives (i.e., metakaolin and silica fume). Thus, in cases where higher workability is required for clay-based AACs, mineral admixtures such as fly ash or chemical admixtures such as superplasticizers can be incorporated to improve the workability. Recently, Borçato et al. [46] replaced metakaolin with quarry dust up to 40% for geopolymer production and found that the compressive strength ranged between 45 and 60

MPa. They also realized that the increased content of quarry dust decreased the area spread of the different geopolymer mixtures. A similar trend was reported by Amin et al. [47] where the authors replaced slag with metakaolin up to 40% for the production of geopolymer concrete. Another study conducted by Li et al. [48] evaluating the effect of graphene oxide (GO) on the fluidity of fresh metakaolin-based geopolymer showed the decrease ranged from 228 to 146 mm with increased content of GO up to 0.5%. Kaze et al. [30] replaced metakaolin with meta-halloysite (obtained calcined halloysite at 700 °C) up to 50 wt%. They found that the increased content of meta-halloysite increased the flowability of fresh geopolymer paste. This was attributed to particle size and the specific surface areas of both solid precursors. A similar trend was also reported by Bheel et al. [49] where the authors evaluated the synergetic effect of metakaolin (MK) and groundnut shell ash (GSA) on fresh fly ash-based geopolymer concrete cured at room temperature. The recorded slump flow diameter decreased from 700 to 550 mm and 700 to 580 mm respectively with increased content of MK and GSA up to 20 wt%. While the combined effect of both additives decreased the slump in comparison with each substituent. Kumar Gautam and P. Alam [50] also reported the increased value of slump of concrete mixing using bottom ash blended with metakaolin. Jithendra et al. [51] investigated the effect of the molarity of alkaline solution (1.5, 1.75, and 2 M) on the workability of fly ash-based geopolymer mortar incorporating metakaolin up to 20 wt%. From their results, they found that samples made with 1.5 M alkaline solution gave good workability and ensured high performance.

2.1.2 *Setting times*

Setting time is one of the key parameters that are related to the behaviour or reactivity of solid precursors used for the synthesis of AACs. Several studies used the Vicat needle to evaluate the setting times of AACs produced from different types of clay as shown in Table 1. These studies have indicated that the setting times of AACs are highly dependent on the nature of the solid precursor (i.e., mineralogy and chemistry), curing temperature, and composition of alkaline or acid solution [7]. For example, Peng et al. [52] investigated the effect of slag replacement on the hardening of alkali-activated metakaolin-slag cured at room temperature. Findings from the study showed that increasing the content of slag resulted in a decrease in the initial and final setting times compared to when pure metakaolin was used as the precursor. The reduction in the setting times as a result of the presence of slag can be linked to the slag being rich in calcium oxide (i.e., 38.28 wt%), thereby resulting in the formation of the calcium silicate hydrate phase. A similar observation was made by Driouich et al. [53] who had optimized metakaolin-blast furnace slag-based geopolymer synthesis using mixture design and response surface methodology (RSM). They found that the setting time decreased from 819 to 216 min with increased content of metakaolin up to 0.5. Ranjbar et al. [54] demonstrated the accelerated setting time of 3D printed geopolymer using calcined halloysite (meta-halloysite (MHA)) at temperatures ranging between 30 and 1,000 °C in comparison with formulations using raw halloysite (HA) as reported in Figure 2. This accelerated setting was attributed to the formation of an amorphous phase upon heating which easily reacted in an alkaline medium and improved the reactive content in fly ash used main material for geopolymer synthesis resulting in a shorter setting. Hasnaoui et al. [55] replaced metakaolin with seashell waste up to 30 wt% and observed the setting decreasing from 450 to 275 min. They concluded that the release of Ca^{2+} from waste material could react easily with hydroxyl ions from an alkaline activator to form portlandite and CSH phase responsible short setting [56]-[57]. Jean Noel Yankwa Djobo and Dietmar Stephan [58] used calcium hydroxide and calcium silicate up to 9 wt% to reduce the setting time of metakaolin-based phosphate cement. The reduced setting times were attributed to Ca^{2+} from calcium hydroxide and calcium silicate which accelerated the setting. Nemaleu et al. [59] obtained the long setting times from meta-halloysite-based geopolymer binders when incorporating raw peel banana ash up to 20 wt%. The initial and final setting times were ranged from 68 to 127 min and 90 to 166 min, respectively. Such an increase in setting time was attributed to the release of alkali species from banana peel ash which hindered the geopolymerization reaction resulting in a long setting. A similar trend was reported in another study replacing fly ash with metakaolin up to 50 wt% using an acidic medium (phosphoric acid) [60]. Later, Nemaleu et al. [61] evaluated the effect of quarry dust (granite and basalt) content (up to 20 wt%) on fresh properties of geopolymer binders using calcined clayey laterite soil at 600 °C. They reported that the initial setting time increased from 41 to 145 min and 85 to 131 min, respectively, when added granite and basalt wastes up to 20 wt%. The increased setting recorded was attributed to the crystalline nature of both quarry wastes used as additives which are less or non-reactive in comparison with calcined clayey laterite containing metakaolin that was formed upon heating of laterite soil.

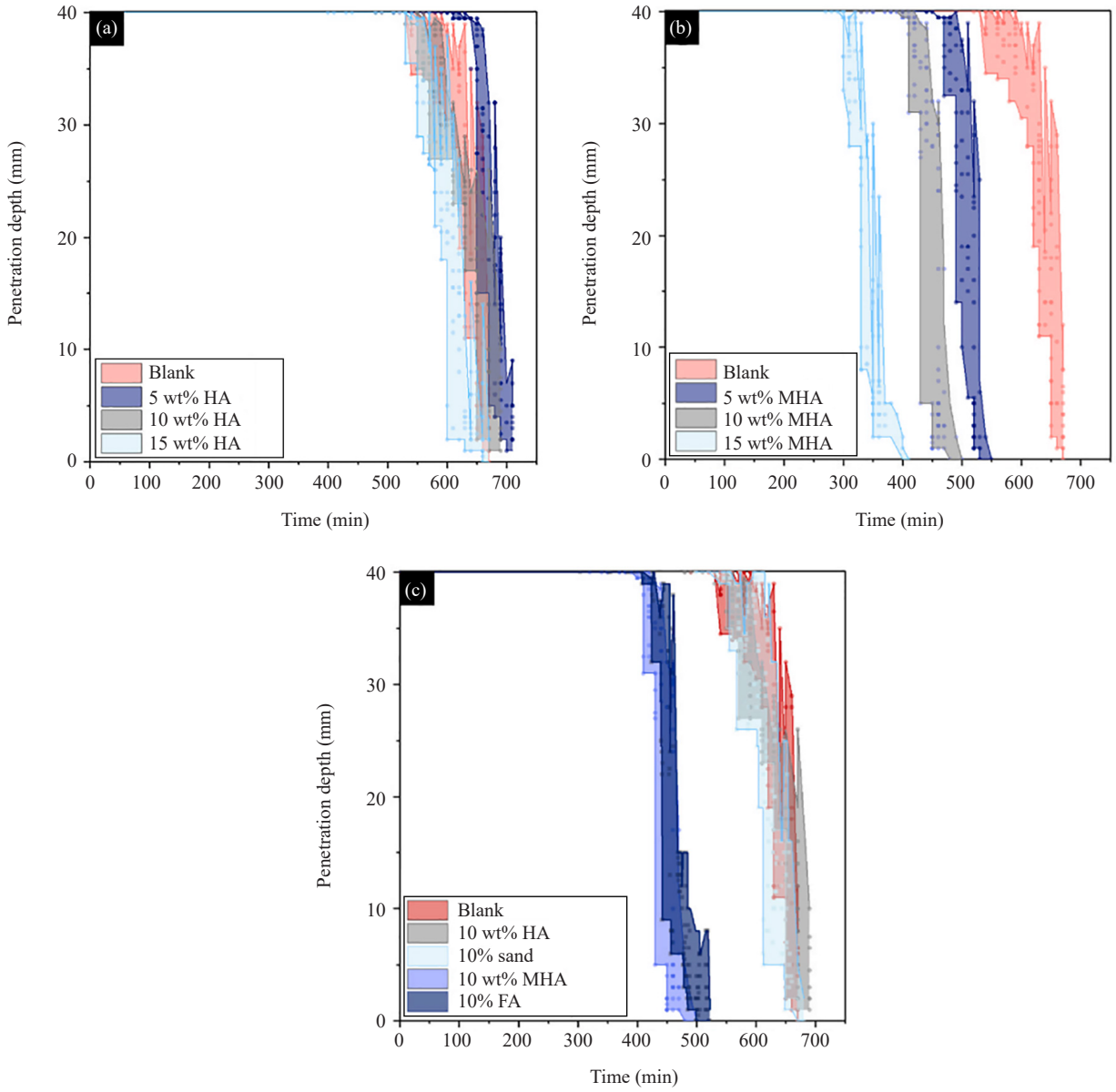

Figure 2. Vicat setting time of geopolymer mortars containing different amounts of a) HA and b) MHA; c) comparison of setting time of geopolymer mortars containing 10% HA/MHA with reference compositions including a similar proportion of FA and sand [54]

Another finding of Boum et al. [62] on metakaolin-based AACs where bauxite was incorporated resulted in an increase in the setting time from 150 to 240 minutes. The extension of the setting time when bauxite was used can be attributed to the non-availability of aluminum from bauxite during the dissolution step of geopolymerization that delayed the setting. Bayiha et al. [63] also reported that the incorporation of calcined powder in thermally activated halloysite delayed the setting when applying an alkali activator with a concentration of 8 M, 10 M, and 12 M. Zhang et al. [64] studied the reactivity of AACs made with calcined halloysite and subjected to a dry and moist environment. Findings from the study showed that increasing the curing temperature from 25 to 90 °C decreased the setting times (initial and final) from 208 minutes to 15 minutes and 603 minutes to 25 minutes, respectively. On the other hand, the initial and final setting time decreased from 220 minutes to 15 minutes and 609 minutes to 31 minutes, respectively in a moist environment. Kaze et al. [65] studied the effect of an alkaline activator on the setting of calcined halloysite and iron-rich laterite at 600 °C. The results revealed that the high alkalinity promotes high dissolution and accelerates the polycondensation step thus making the setting time shorter. Other studies conducted on the influence of calcination

temperature on the reactivity of some clayey materials such as kaolinite and halloysite demonstrated that increasing the calcination temperature between 550 and 850 °C improves the reactive or amorphous content and thus reduces the setting time when applied to an alkaline solution [19], [54], [66].

Table 1. Setting times of previous works carried on geopolymer composites from literature

Solid precursors	Activators	Setting time (min)
Slag/metakaolin (100/0, 80/20, 60/40, and 40/60) [52]	Sodium silicate (SiO_2/Na_2O = 1.4, 1.6, 1.8, and 2.0)	Decreased from 10 h to 100 min
Fly ash blended with 5, 10, and 15 wt% of halloysite (HA) and meta-halloysite (MHA) [54]	8 M NaOH with Sodium silicate in ratio weight of 15/2	-Decreased from 700 to 600 min for samples made with HA -Decreased 700 to 400 min for samples made with MHA
Blast furnace slag/metakaolin in ratios 0.3, 0.4, and 0.5 [53]	NaOH and sodium silicate in a ratio of 2	Reduced from 819 to 216 min
Metakaolin and fly ash (80/20, 70/30, and 50/50) [60]	Phosphoric acid	Increased from 10 to 800 min and 25 to 1,300 min, respectively for initial and final setting times
Metakaolin/slag (100/0, 90/10, 80/20, and 70/30) [56]	NaOH and sodium silicate in a ratio of 2/1	Decreased from 600 to 180 min
Calcined laterite mixed quarry waste (basalt and granite up 20 wt%) [61]	NaOH and sodium silicate in a ratio of 1/1	-Increased from from 41 to 131 min and 95 to 272 min with increased content of basalt up to 20 wt% respectively for initial and final setting times -Increased from from 85 to 145 min and 148 to 266 min with increased content of granite up to 20 wt% respectively for initial and final setting times
Metakaolin and bauxite (100/0, 90/10, 80/20, 70/30, and 60/40) [62]	Sodium silicate (SiO_2/Na_2O = 1.5 and H_2O/Na_2O = 10)	2 h 30 min to 4 h with increasing of bauxite up 50 wt%
Calcined halloysite/lime (100/0, 85/15, 70/30, and 60/40) [63]	Sodium silicate and NaOH solutions (5, 8, and 10 M) in a ratio of 1/1	122 to 304 min, and 67 to 180 min, respectively, for 5 and 10 M
Laterite/meta-halloysite (100/0, 80/20, 70/30, and 50/50) [65]	Sodium silicate (SiO_2/Na_2O = 0.75, 0.95, and 1.04)	140-80 min, 100-40 min, 90-30 min, and 60-20 min, respectively
Fly ash/metakaolin containing H_2O_2	Sodium silicate (SiO_2/Na_2O = 1.3)	Decreased from 300 to 100 min, and 340 to 140, respectively for initial and final setting times
Volcanic ash/metakaolin in ratios (0.20, 0.25, 0.33, and 0.50) [67]	Sodium silicate (SiO_2/Na_2O = 3.08)	Decreased from 1,530 to 750 min, and 1,260 to 345 min respectively for final and initial setting times
Spent catalyst/metakaolin (0-20 wt%) [68]	Sodium silicate (SiO_2/Na_2O = 1.5)	193-272 min and 270-360 min
Volcanic-ash/ metakaolin (100/0, 95/5, 90/10, 85/15, 80/20, and 75/25) [69]	Sodium silicate (SiO_2/Na_2O = 1.1 and 1.4)	560-160 min and 220-125 min respectively for ZD and ZG volcanic-ash types containing MK at different dosages
Nano-SiO_2 metakaolin [70]	Sodium silicate (SiO_2/NaO_2 = 1-2)	185 to 343 min and 225 to 390 min, respectively for initial and final setting times
Nano-SiO_2 metakaolin [71]	Sodium silicate/sodium hydroxide = 2	360 to 45 min

2.2 *Mechanical properties*

2.2.1 *Compressive strength*

The mechanical properties of AACs can be linked to the physicochemical properties of solid precursors and the nature of the alkaline solution as well as the setting time. Hence, to improve the properties of the end products some secondary precursors can be added as additives at different proportions to enhance the reactive phase of the main solid precursor. Tchakoute et al. [72] altered volcanic ash-based AAC by incorporating metakaolin up to 40%. Findings from the study showed that the use of metakaolin up to 20% replacement of the volcanic ash yielded the maximum compressive strength of 52 MPa. Rajamma et al. [73] combined biomass fly ash (BFA) with metakaolin in proportions of 80/20 and 60/40 and used an alkali solution with concentrations ranging between 10 M to 18 M to produce AACs.

The results from the study showed that the compressive strength increased from 14.24 MPa to 36.84 MPa and 18.09 MPa to 38.34 MPa for AACs composed of volcanic ash/metakaolin of 80/20 and 60/40, respectively. Findings from the study also showed that the compressive strength of the AACs increased with a higher concentration of the alkali solution which favoured the high degree of polycondensation.

Zulkifly et al. [74] combined metakaolin and fly ash at a ratio of 1/1 as solid precursors for AAC. For the synthesis, monoaluminium phosphate (MAP) and aluminum dihydrogen triphosphate (ATP) were added as a source of aluminum phosphate at 1 and 3 wt%, respectively. The highest compressive strength recorded ranged between 55.5 MPa and 63.7 MPa for the samples incorporating 1 wt% of the source of aluminum phosphate. Liu et al. [75] produced an AAC from a mixture of red mud (RM) and coal metakaolin (CMK) in proportion 70/30 at different Na/Al ratios (0.8 to 1.3). Results from the study showed that the compressive strength of all the AACs increased with curing ages of 7 days to 28 days. It was also reported that the Na/Al ratio of 1.0 yielded better mechanical performance at all different ages. Peng et al. [52] simultaneously evaluated both the effects of silica moduli and the effect of curing temperature on the slag replacement in metakaolin up to 80 wt%. From their study, the use of an activator with a silica modulus (SiO_2/Na_2O) of 1.4 and curing at 70 °C yielded the highest compressive strength at early ages. At a later age (i.e., 28 days), the use of an activator with a silica modulus (SiO_2/Na_2O) of 2 yielded the highest compressive strength for AACs made with slag as a replacement of metakaolin in the range of 50% to 100%. It has been discovered that the silica modulus of the activator solution affects the physical characteristics of samples of geopolymer paste. The impact of the SiO_2/Na_2O molar ratio on the bulk density and water absorption of geopolymer paste samples was investigated by previous studies [76]-[77] demonstrating that while bulk density is not significantly affected by changes in the SiO_2/Na_2O ratio, water absorption increases with increases or decreases in the SiO_2/Na_2O ratio beyond the optimum. Hence the silica modulus appears as one of the key parameters governing the end properties of AACs.

Nana et al. [78] used mechanical activation to improve the reactivity of pegmatite, which is used as a solid precursor for geopolymer synthesis. They varied the milling time from 15 to 90 min. The microstructural characterization revealed that milling pegmatite reduced undissolved/unreacted particles while increasing non-bridge particles. The formation of more reaction products in scanning electron microscope (SEM)/Energy Dispersive Spectroscopy (EDS) and transmission electron microscope (TEM) highlights the fineness of pegmatite particles. The compressive strength of geopolymer binders increased from 22.3 to 51.6 MPa after 0-60 minutes of milling. From their study, 12.5 wt% of metakaolin was added.

Metekong et al. [19] combined volcanic ash and calcined laterite clay in different proportions of 80/20 and 60/40 alongside an alkaline solution composed of sodium silicate and sodium hydroxide to produce AACs. After 28 days of curing, they observed a compressive of approximately 49 MPa for AAC made with calcined laterite clay as a 40% replacement of volcanic ash. Findings from the study also showed that the compressive strength of the AACs increased with increased curing temperature (28-80 °C) which favoured the high degree of polycondensation [8], [22], [79]. In the same vein, Kaze et al. [65] altered calcined iron-rich laterite up to 50 wt% of calcined halloysite and studied the effect of molarity of alkaline solution on the properties of AACs. The results from the study showed that the incorporation of calcined halloysite improved the reactive phase thereby resulting in enhancement of compressive from 12 MPa to 45 MPa. Zhu et al. [80] improved the mechanical properties of MK-based geopolymer with the incorporation of slag up to 40 wt%. The compressive strength increased and reached the maximum at 62 MPa when 30 wt% of slag was added. This improvement is in agreement with other studies incorporating different secondary materials sources at different dosages like slag [56]-[57], [81]-[83], metakaolin [24], [51], [81], [84]-[85], fly ash [60], [86]-[88], granite-quartz-pegmatite [89]-[90], marble [18], nano silica fume [91], bottom ash [50], graphene oxide [48], volcanic ash [92], and hematite [93]. Han et al. [94] simultaneously evaluated the effect of silica moduli, the influence of SiO_2/Na_2O, and the effect of the liquid-to-solid ratio on the MK replacement in municipal solid waste incinerated fly ash (MSWIFA) up to 40 wt%.

Jaji et al. [56] altered metakaolin-based AAC by incorporating slag up to 30%. Findings from the study showed that the use of slag up to 30% replacement of the metakaolin yielded a maximum compressive strength of 32 MPa. Nemaleu et al. [61] combined calcined laterite clay with waste granite and basalt powders in proportions of 95/25, 90/10, 85/15, and 80/20, and used an alkali solution to produce AACs. The results from the study showed that the compressive strength decreased from 36 MPa to 8 MPa and 40 MPa to 6 MPa for AACs composed of calcined laterite/granite and calcined laterite/basalt, respectively. This loss in strength explains the inert nature of these powders in

an alkaline medium. A similar trend was pointed out by Venyite et al. [95] where the authors combined metakaolin, unheated laterite, and basalt powder at different dosages. Shilar et al. [96] also reported the decreased strength recorded on metakaolin-based geopolymer blended with marble up to 40 wt%. Tian et al. [97] produced porous metakaolin-based geopolymer incorporating MSWIFA up to 60 wt%. The obtained mechanical performance decreased from 12 to 5 MPa with the rise of MSWIFA content. Hence, adding the non-reactive secondary source material was not beneficial for the strength development during the geopolymer synthesis. This is because, instead of reacting, these materials tend to reduce the reactive phase and hinder the geopolymerization reaction.

Liu et al. [75] produced an AAC from a mixture of red mud (RM) and coal metakaolin (CMK) in proportion 70/30 at different Na/Al ratios (0.8 to 1.3). Results from the study showed that the compressive strength of all the AACs increased with curing ages of 7 days to 28 days. It was also reported that the Na/Al ratio of 1.0 yielded better mechanical performance at all different ages. In a similar study [98], MSWIFA was combined with metakaolin at a ratio of 90/10. The outcome of the study showed that the incorporation of 10 % of metakaolin to MSWIFA increased the compressive strength by about 200% compared to that reference AAC (i.e. without MK). The improvement of performances at advanced ages was linked to the formation of the ettringite phase from the reaction between $CaSO_4$ contained in fly ash and aluminate species from metakaolin. Lemougna et al. [99] in their investigation replaced calcined laterite with calcium carbonate and slag up to 20 and 50 wt%, respectively, and the compressive strength. The results indicated that the maximum compressive strength achieved at 28 days is for AACs incorporating calcium carbonate and slag as a replacement of calcined laterite at a ratio of 20% and 50%, respectively.

2.2.2 *Flexural strength*

The flexural strength of AACs can be linked to the cohesion or connectivity and bonding strength between different components within the matrix of the composites. Kamseu et al. [89] evaluated the effect of fine aggregates (quartz, granite, and pegmatite) on the mechanical properties of metakaolin/metahalloysite-based AACs. The findings from the study showed that the 28th-day flexural strengths increased from 26 MPa to 36 MPa. The enhanced flexural strength in the AACs was linked to the formation of H-C-S and H-C-A-S with H-M-A-S phases within the matrix which yielded better polycondensation and allowed the formation of a stronger matrix. Hence, it was found out that despite feldspar not containing the same amount of amorphous phases as pumice and waste glass, it is mainly constituted of fine particles which is beneficial for strength development. Similarly, Nemaleu et al. [100] replaced metakaolin with semi-crystalline materials (i.e., kyanite having a particle diameter of 80, 200, and 500 µm) in the range of 70-85 wt%, for the synthesis of AACs and heated between 1,050 and 1,250 °C. The results from the study showed that the incorporation of kyanite powder enhanced the flexural strength as shown in Figure 3. It is observed that larger amounts of kyanite induced higher particle density within the matrices, resulting in the improvement of flexural strength at temperatures below 1,200 °C. In the same vein, Nana et al. [101] used a microstructural approach to investigate the effect of particles size distribution of fine aggregates (granite and pegmatite composed as follows: A = 100 wt% of $\phi \leq 63$ µm; B = 50 wt% of $\phi \leq 63$ µm + 50 wt% of $8 \leq \phi \leq 125$ µm; C = 50 wt% of $\phi \leq 63$ µm + 50 wt% of $125 \leq \phi \leq 200$ µm; and D = 33 wt% of $\phi \leq 63$ µm + 50 wt% of $80 \leq \phi \leq 125$ µm + $125 \leq \phi \leq 200$ µm) on the strength development. They realized that the gradual addition of fine and coarse particles with coarse ones of particle size between $80 \leq \phi \leq 125$ and $125 \leq \phi \leq 200$ µm at the proportion 1:1 improved the flexural strength from 30 to 36 MPa. This supports the idea that the efficiency of the geopolymerization and the particle packing work synergistically. The particle size distribution influences the properties of the pastes and promotes packaging. As a result, it alters the material's rheological properties during the mixing process, as well as the mechanical properties of the hardened material when non-reactive particles are present. Based on this, it can be considered that sample made with smaller particle sizes is expected to have a higher reactivity than those made with high ones. Specifically, the extra sodium aluminosilicate hydrate (N-A-S-H) gels are formed at the matrix-aggregate contact. Kamseu et al. [102] produced geopolymer with low metakaolin incorporating different types of fine aggregates such as quartz sand, nepheline syenite, and ladle slag up to 60% and then investigated the flexural strength up to 180 days. They found an increase in mechanical performance from 4 to 6 MPa, 4 to 9.1 MPa, and 4 to 10 MPa, respectively, for samples made with quartz sand, ladle slag, and nepheline syenite between 28 and 180 days of curing. Such recorded improvement was attributable to fine particles which enhanced the interfacial zone for the design of optimum-grade and high-performance composites. Finely ground semi-crystalline materials can dissolve in an alkaline medium, enriching the medium with Si and Al oligomers and reinforcing the geopolymer structure, which is most likely responsible for the

improved mechanical performance observed [89], [102]-[103].

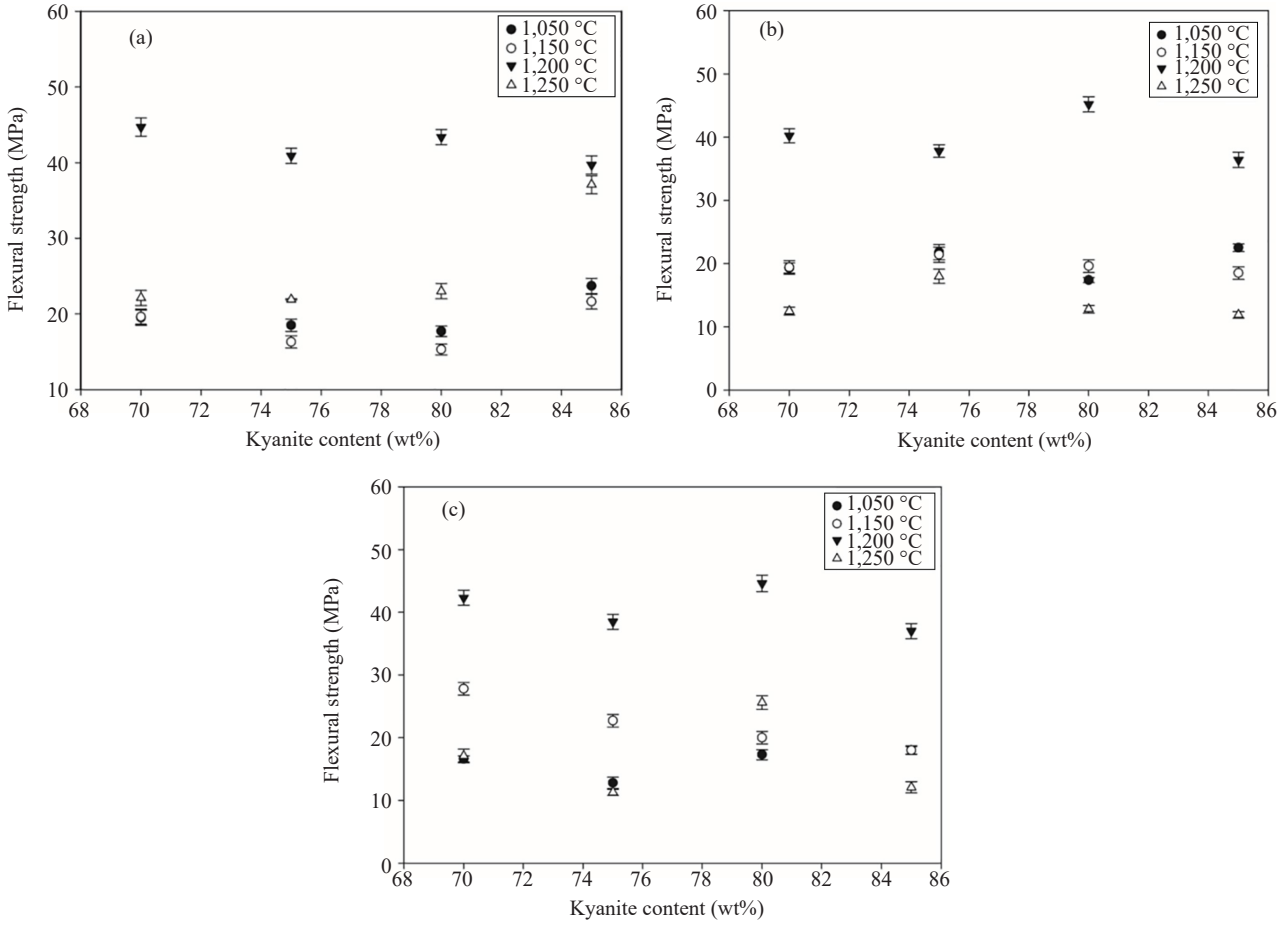

Figure 3. Flexural strength: (a) RB series (samples made with kyanite having 80 µm), (b) RC series (samples made with kyanite having 200 µm), and (c) RD series (samples made with kyanite having 500 µm) [100]

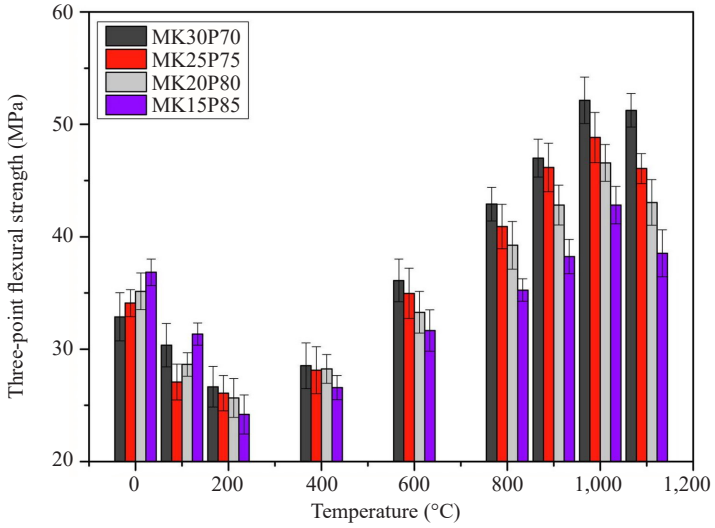

Figure 4. Variation of the three-point flexural strength of metakaolin-based geopolymer blended with pegmatite at different dosages heated at various temperatures [104]

Nana et al. [104] replaced metakaolin with pegmatite in the range of 70-85 wt% for the geopolymer production and the resulting products were heated up to 1,000 °C. The values of flexural strength were ranged between 46 and 51 MPa. The high performance was achieved on samples heated at 1,000 °C, related to densification, vitrification, formation of new phases, etc. occurring upon heating which increased particle connectivity and facilitated the strength increase (Figure 4). The loss of flexural strength above 1,000 °C was related to the soda-rich gel rapidly transforming to a low-viscosity liquid phase. The same authors [105] blended pegmatite with 12-15 wt% of metakaolin (MK) and metahalloysite (MH) and found that the values of flexural strength ranged from 32 to 34 MPa with 15 wt% of MK and 38 to 42 MPa with 12 wt% MH added, respectively.

2.3 *Durability properties*

2.3.1 *Porosity*

Porosity in composites represents a set of voids or pores present in the matrix that can be filled with fluids. The presence of voids/pores in composites such as AACs has a direct influence on their corresponding durability properties. Similarly, porosity can be linked to the mechanical performances of composites. Gao et al. [106] studied the effects of metakaolin/alkaline activator ratios (0.97, 1.03, 1.10, and 1.19) and nano-silica additions (1, 2, and 3%) on the porosity of metakaolin-based AACs. Observations on immersed samples for the water absorption test indicated that the incorporation of 1% of reactive nano-silica favoured the reduction in pores within the matrices of different fabricated AACs with a curing time of up to 60 days. The optimum result of porosity was obtained on a sample prepared with a metakaolin/alkaline solution ratio of 1.03. On the contrary, the findings by Cheng et al. [107] where metakaolin was replaced with waste catalyst up to 40 wt% showed that the porosity of the AACs increased in the presence of the waste catalysts. Nonetheless, the optimum content of the waste catalyst to be used was suggested to be 10% as it resulted in similar porosity as that of metakaolin-based AACs without any additives.

In the study by Buchwald et al. [108], different fillers were incorporated at various proportions into AACs, and the thermal and microstructural properties of the resulting AACs up to 1,000 °C were evaluated. Based on their findings, applying a temperature of 1,000 °C was beneficial in the reduction of porosity in all the AACs blended with fillers. The most reduction was observed on AACs containing 2% of quartz and 50% of clay fillers. The reduction in the porosity at the elevated temperature (i.e., 1,000 °C) can be linked to the sintering effect which resulted in a physicochemical transformation in the matrices thereby making the structure compact with few accessible voids. Bignozzi et al. [109] used the mercury intrusion porosimetry (MIP) method to evaluate the distribution of pores contained in AACs made with a mixture of metakaolin and ladle slag in proportion 75/25, 50/50, 60/40, 70/30, and 80/20. Findings from the study indicated that incorporating metakaolin as a 20% replacement of the ladle slag AAC resulted in more reduction in the intruded volume from 330 to 140 mm^3/g. It was related to the progressive addition of MK, which extended the geopolymer network, resulting in the formation of a densified structure.

Nemaleu et al. [100] studied the effects of metakaolin/kyanite ratios and pores size of kyanite (80, 200, and 500 µm namely RB, RC, and RD respectively) on the porosity of metakaolin-based AACs. Observations on immersed samples for the water absorption test indicated that the incorporation of fine particles (80 µm) of kyanite favoured the reduction in pores within the matrices of different fabricated AACs with heating temperature. The apparent porosity ranged from 36 to 19, 34 to 21, and 31 to 37 vol% for the RB, RC, and RD series, respectively.

Nana et al. [101] used the mercury intrusion porosimetry (MIP) method to evaluate the distribution of pores contained in AACs made with a mixture of metakaolin and granite or pegmatite in proportions. Findings from the study indicated that incorporating pegmatite or granite replacement of the metakaolin AAC resulted in more reduction in the intruded volume. When pegmatite is utilized as a solid precursor, the various classes of particles demonstrate a continuous decrease in pore size and cumulative pore volume. The better mechanical performance obtained with the pegmatite specimens compared to the granite specimens can be explained by the combined action of the creation of adequate viscous gel to embed the particles and fill capillary and the efficacy of particle packing. With particular attention, it can be seen that as packing density increases, pores' size and cumulative volume decrease. Additionally, while there are a few tiny capillary porosity bands in the granite series specimens, the solid solution-based geopolymer composites are primarily characterized by monomodal bands of mesoporosity, which indicate extremely low porosity interconnectivity resulting in a low value of water absorption and porosity obtained.

2.3.2 *Water absorption*

Similar to the porosity of composites, water absorption is a good indication of the durability performance of AACs as it shows the ease with which various determinantal materials can go into and through the composites. Several studies [110]-[111] demonstrated that the water absorption values of heated AACs increase with the rise of heating temperature from 25 to 1,000 °C. The increase in water absorption was attributed to the appearance of open voids and microcracks within the matrices after undergoing heating related to the degradation of the binder phase responsible for the better cohesion between different components. Thus, after heating the presence of these voids would allow high retention of water compared to the unheated AACs [17], [79], [112].

Nemaleu et al. [113] mixed metakaolin with groundnut ash in weight ratios of 90/10, 80/20, and 70/30 alongside two alkaline solutions with 8 and 10 M for the production of AACs. The findings at 28 days showed that AACs made with lower concentration (i.e., 8 M) alkaline solution exhibited higher water absorption ranging between 7-25% which also increased aggregates replacement and decreased with curing days from 7 to 28 days. The higher water absorption was suggested to be due to either the possible leaching of groundnut powder ash when samples were immersed in water and became lighter or to more pronounced voids that could retain much water. A similar trend was reported by Xu et al. [94] who replaced metakaolin with MSWIFA up to 40 wt% and observed the increased porosity from 19 to 30%. Nonetheless, the findings by Kaze et al. [65] showed that water absorption can be reduced up to 50% in iron-rich laterite-based AACs by incorporating fine meta-halloysite up to 50 wt%. The incorporation of the fine meta-halloysite was found to improve the Si/Al ratios making the AAC matrix less heterogeneous and more compact. A similar trend was reported by other studies incorporating different secondary sources such as quarry dust [46] where the authors observed a decrease in water absorption from 43 to 27% with increased content of quarry dust up to 40 wt%.

Certain factors affect the porosity and water absorption of AACs, such as alkaline solution types used, liquid to solid ratio for the AACs synthesis [96], [114]. Nouping et al. [93] investigated the effect of alkaline sources on the reactivity of metakaolin/hematite- and laterite-based geopolymer using Na or K activators. They reported that, when the potassium silicate activator was used, the porosity reached 43% and 31% in the case where the sodium silicate activator was applied. The authors concluded that such difference could be linked to the higher crystallinity of the powder activated with sodium silicate displaying weak porosity compared to those activated with potassium silicate which were heterogeneous allowing high porosity.

2.3.3 *Chloride ion penetration*

A chloride ion penetration test is used to assess the ease at which chloride ions that are favourable to corrosion can penetrate the composites. Studies have indicated that the mechanism of chloride ions transport is based on the following factors: water diffusion, impregnation, and capillary absorption. Compared to AACs made with a precursor such as fly ash and slag, there is limited knowledge on the chloride ion penetration of clay-based AACs. Nonetheless, Fu et al. [115] studied the chloride penetration resistance of AACs made with fly ash and metakaolin as precursors alongside two different alkali activators. Findings from the study showed that using a lower liquid-to-solid ratio with refined pores in fly ash-based AACs reduces the chloride diffusivity compared to metakaolin-dominant AACs. It was also found that AACs made with Na-activators exhibited higher resistance to chloride penetration than those from K-activators. This difference might be attributed to the fact that the Na-AACs showed a higher geopolymerization reaction, higher mechanical performance, and lower porosity compared to the K-AACs. With limited studies on the chloride ion penetration in clay-based AACs, more studies are recommended in this area.

2.3.4 *Resistance in aggressive environment*

Jin et al. [116] investigated the acid resistance of metakaolin-MSWI fly ash blend in simulated acid rains with various pH (i.e., 3, 4, and 5). The acid resistance was evaluated in terms of the resulting strength at it was found that the reduction in pH from 5 to 3 resulted in a loss in strength in the range of 7.4% to 13%. Duan et al. [117] their study compared the acid exposure of Portland cement and fly ash-metakaolin AACs in an acidic mixture of sulfuric acid (2%) with hydrochloric acid (2%). After 56 days of exposure, the AACs showed good resistance compared to that of PC.

Kuang et al. [81] investigated the effect of seawater and deionized water on the properties of metakaolin/slag-

based geopolymer. After investigating for a longer period, they observed that the difference in terms of flexural and compressive strength recorded in both media was small as seen in Figure 5. This seawater resistance was explained by an increased content of Ca^{2+} promoting the dissolution of Al and Si monomers, reducing the need for the required Na_2O concentration to hydrate precursors. This results in the formation of an additional binder phase namely C-(A)-S-H type in metakaolin/slag blends making these samples denser with few accessible voids and improving the mechanical performance. The same authors evaluated the chloride migration on the same specimens. It was observed a gradual decrease of chloride migration coefficient with increased content of slag. This mitigation of chloride penetration was related to the coexistence of both binder phases, C-A-S-H or C-S-H and N-A-S-H, allowing the development of a strong matrix.

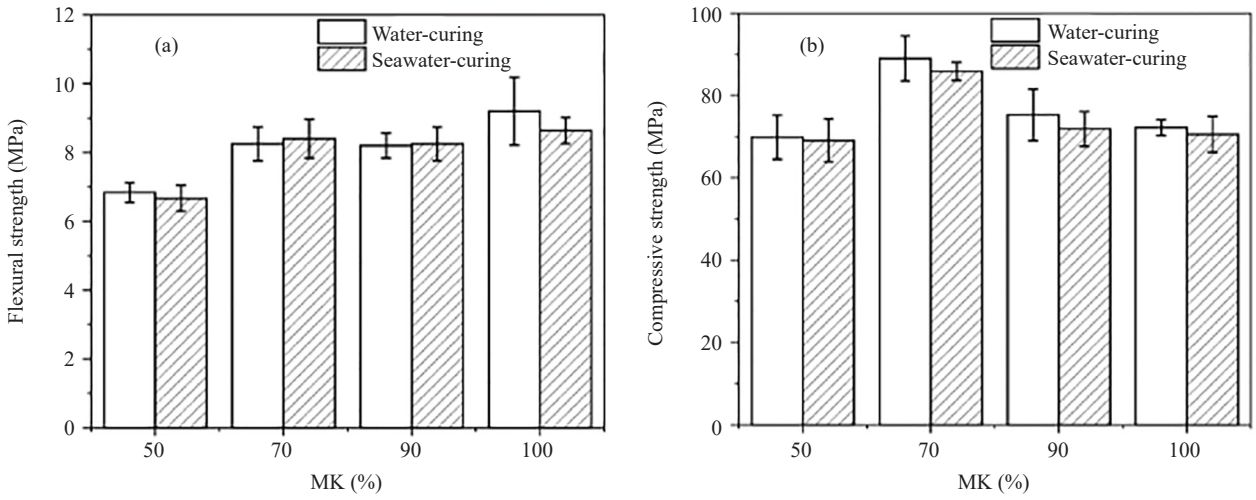

Figure 5. Mechanical properties of geopolymer composites at 90 days: a) flexural strength and b) compressive strength [81]

Similarly, Sontia et al. [19] improved the reactivity of volcanic ash by incorporating the calcined laterite up to 40 wt% followed by the curing of the AACs at 28, 60, and 80 °C. After 20 weeks of exposure in an acidic medium, they recorded the following mass changes of 8.29/7.05/6.63% and 6.22/5.29/4.98%, respectively, for AACs containing 20 and 40 wt% calcined laterites. The produced AACs exhibited better resistance to the acidic medium compared to that of PC composites subjected to similar extreme conditions. However, the reduction in the mass and strength of AACs in the acidic environment was linked to the breaking down of Si-O-Al resulting in deterioration of the AACs. This deterioration was more pronounced on AACs cured above room temperature.

2.3.5 *Drying shrinkage*

Linear shrinkage measures the decrease in the dimensions (height and diameter) of the specimens due to the departure of water and the physico-chemical phenomena that take place in the material. It follows that if the excess water contained in the AACs is not consumed during the polymerization, it diffuses out of the surface of the AAC matrix creating pores [118]-[119]. This results in a shrinking of the test specimen and hence the linear shrinkage. Kaze et al. [112] found that the shrinkage of heated metakaolin/metahalloysite-based AACs increased up to 14 and 16%, respectively with higher heating temperatures. This shrinkage was related to the release of bounded chemical water to the geopolymer network leading to the phyisco-chemical transformations that occurred in the matrix resulting in the reduction in the dimension of specimens [120]. For the metakaolin-based AACs heated up to 1,400 °C using dilatometry analysis, Vidal et al. [121] recorded about 20% of total shrinkage. When replacing both metakaolin with ammonium molybdate up to 1.57 wt%, they found that the decrease in shrinkage from 20 to around 5% in both AAC series M1 (metakaolin with SiO_2/Al_2O_3 ratio of 1.38) and M2 (metakaolin with SiO_2/Al_2O_3 ratio of 1.41) exposed at high temperatures. This reduction showed that incorporating ammonium molybdate was beneficial to the morphological

changes that occurred in both matrices on the microstructure and strength development.

To reduce the shrinkage in cementitious materials some additives like sand have been used. It is the case of the findings of Zawrah et al. [122] who investigated the linear shrinkage of metakaolin-based AACs containing 2.5, 5.0, and 7.5 wt% of nano sand heated at 800, 1,000, and 1,200 °C. The results as shown in Figure 6 revealed that the linear shrinkage of the end products decreases with nano sand content. This reduction is linked to closed pores and voids in the matrix accompanied by a decrease in binder formation. Duan et al. [117] compared the thermal shrinkage of ordinary Portland cement and combined fly ash-metakaolin-based AACs exposed at high temperatures up to 1,000 °C. After heating, they realized that Portland cement exposed to high temperatures exhibited high thermal shrinkage values compared to AACs. This indicates better stability of amorphous sodium aluminosilicate hydrate (N-A-S-H) gel compared to that of calcium aluminosilicate hydrate CASH contained in AACs and Portland cement, respectively (Figure 7).

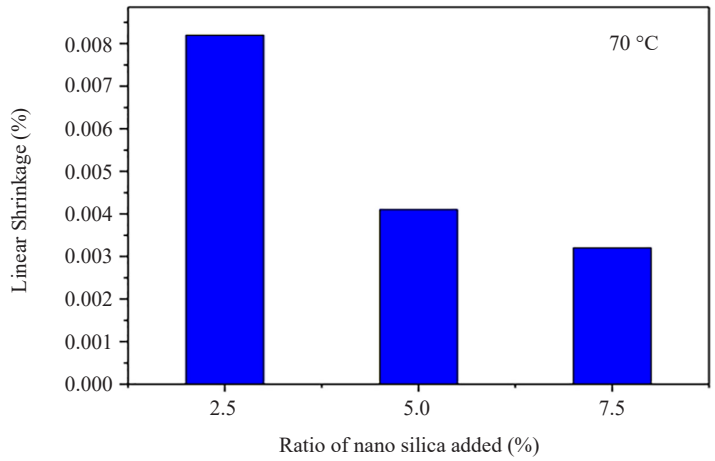

Figure 6. Linear shrinkage of AACs prepared at 70 °C as a function of nano sand ratios [122]

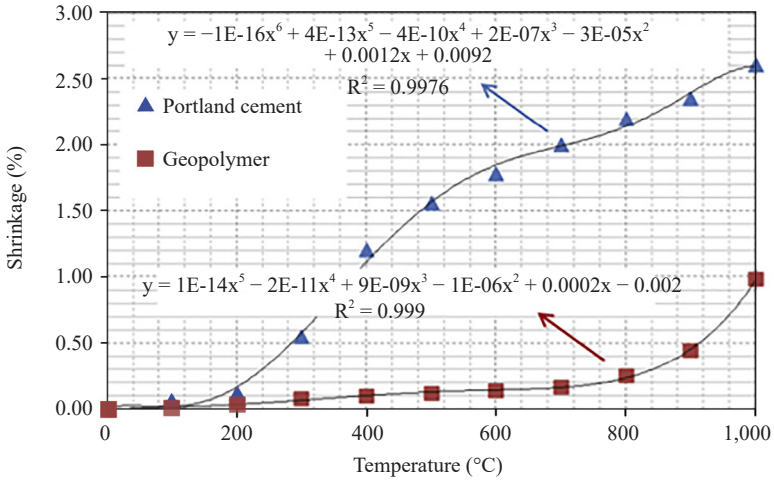

Figure 7. Thermal shrinkage of Portland cement and geopolymer paste with elevated temperatures [117]

2.3.6 *Elevated temperature resistance*

Compared to Portland cement composites, AACs have been found to exhibit better resistance to elevated temperatures making them suitable candidates for specialized applications such as in refractory construction [123]-[127].

Table 2 presents the effects of elevated temperatures on some metakaolin-based AACs. Yaşın and Ahlatc [125] used nano alumina powder to reinforce the Na-metakaolin-based AACs for potential refractory applications. They observed that the compressive strength increased from 30 to 134 MPa with heating temperature up to 1,250 °C. Kamseu et al. [128] in their study used α-quartz and fine alumina powder to stabilize AACs up to 1,200 °C. It was found that the use of α-quartz and fine alumina was beneficial for the end products heated at high temperatures. The heated samples were stable up to 1,100 °C after which a few cracks or fissures were formed at 1,200 °C as shown in Figure 8. The formation of these cracks/fissures can be linked to the sintering stresses related to the newly formed liquid phase and the matrix. It was also found that incorporating α-quartz and fine alumina allows the increase of flexural strength mostly between 800 and 1,200 °C.

Table 2. Effect of elevated temperature on AACs

Precursor	Activators	Heat treatment	Mechanical performances
Metakaolin-fly ash (1/1) [117]	Sodium silicate	20, 100, 200, 300, 400, 500, 600, 700, 800, 900, and 1,000 °C	35 to 39 MPa and 59 to 72 MPa for samples aged of 3 and 28 days heated from 20 to 400 °C. Decreasing from 39 to 2 MPa and from 72 to 25 MPa respectively for Portland cement and AAC.
Metakaolin-pegmatite [104]	Sodium silicate	25, 100, 200, 300, 400, 500, 600, 800, 900, 1,000, and 1,100 °C	15-56 MPa and 20-82 MPa respectively for flexural strength and compressive strength from 25 to 1,100 °C.
Volcanic ash-fired clay bricks [17]	Sodium silicate	25, 200, 400, 600, and 800 °C	Sample made with 10 wt% of waste fired clay brick gave 33 MPa at 600 °C.
PVA-reinforced metakaolin/fly ash-based geopolymer mortar [87] (Polyvinyl alcohol (PVA) content 0%, 0.2%, 0.4%, 0.6%, 0.8%, 1.0%, and 1.2%)	Sodium silicate adjusted to have SiO_2/Na_2O = 1.3	25, 200, 400, 600, and 800 °C	Furthermore, compared to the geopolymer mortar without fibers, the inclusion of PVA fibers greatly increased the compressive strengths and flexural strength of the cubic and prism by 50.5%, 29.4%, and 66.3%, respectively, upon exposure to 200 °C.

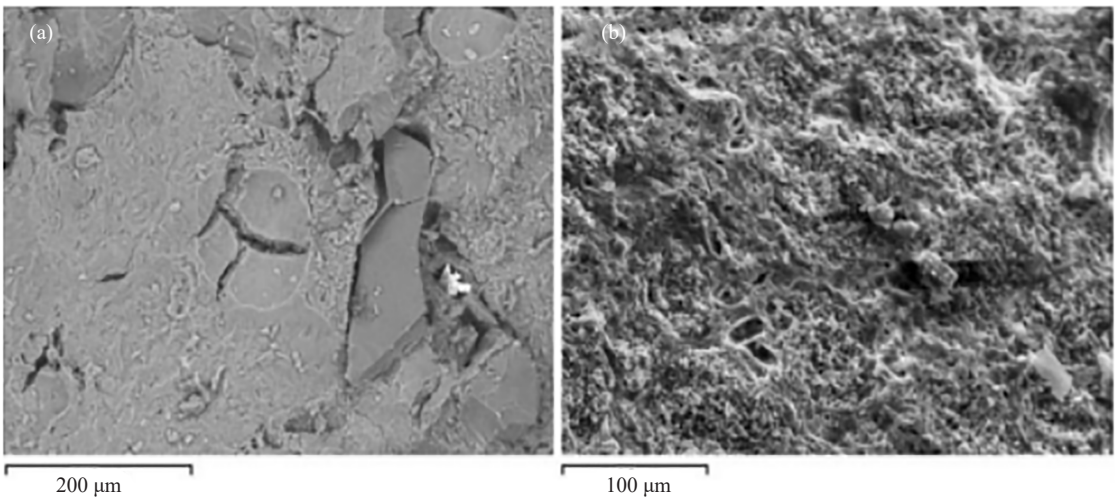

Figure 8. Fractures surface of geopolymer concretes (a: Si-rich; b: Al-rich) at 1,200 °C showing the influence of liquid phase and thermal expansion mismatch on microstructure [93]

Rashad and Ouda [124] partially replaced metakaolin with nano-silica at concentrations of 0.5, 1, 2, 3, and 4 wt% and then heated the resulting AACs from 400 to 1,000 °C. After exposure, they found that the compressive strength of all the samples containing 0.5 wt% of nano-silica increased indicating their stability up to 400 °C. When the temperature was increased from 600 to 1,000 °C, a drastic decrease in compressive strength was observed which was linked to the denaturation of geopolymer binder resulting in low strength. On the other hand, Lin et al. [129] observed a significant

increase in flexural strength on metakaolin-based AACs incorporating the alumina (α-Al_2O_3) powder at different dosages (10, 20, 30, 40, and 50 wt%). This enhancement in mechanical performances was attributed to the reduction in porosity and open voids within the geopolymer matrix and the rise of the density of the end products.

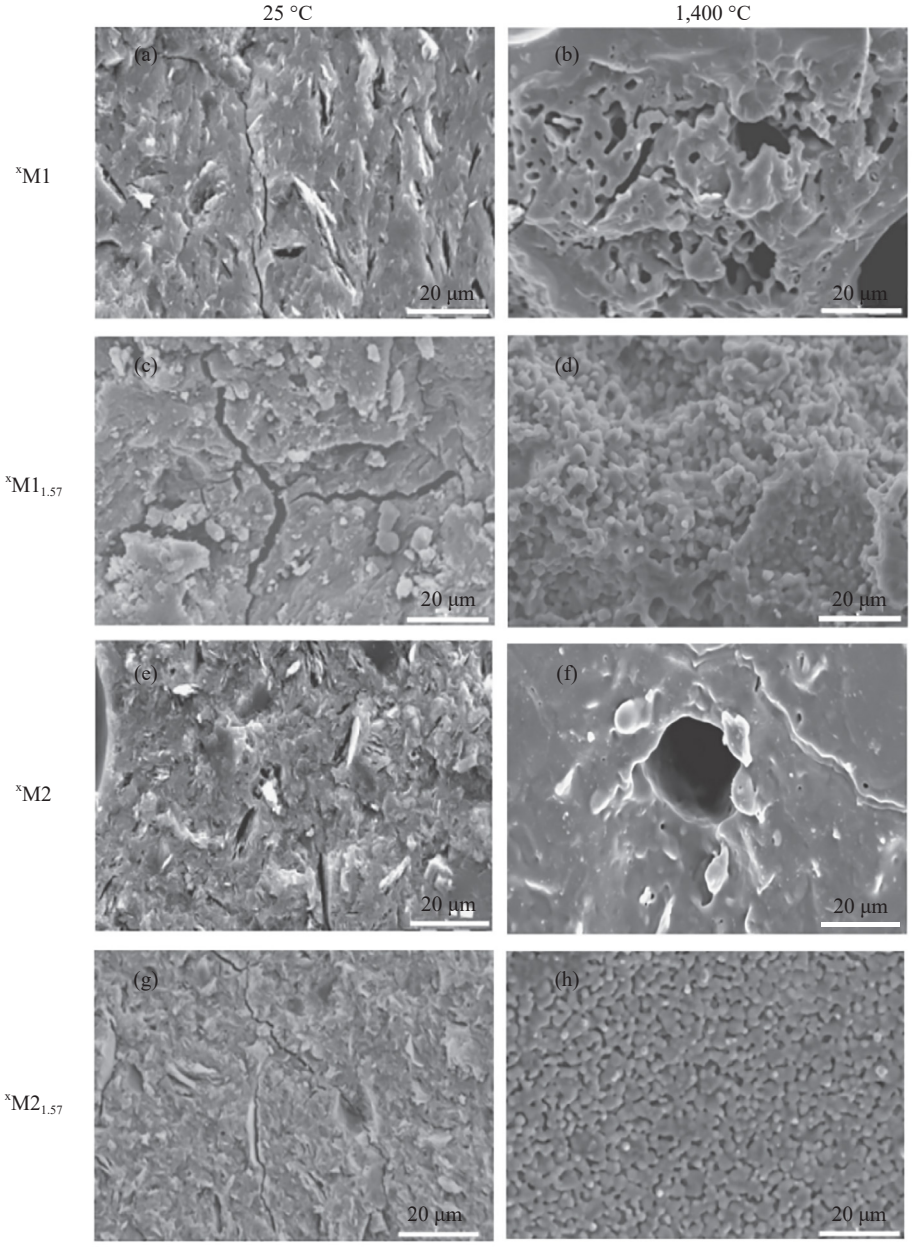

Figure 9. SEM images of AACs from metakaolin M1 (metakaolin with SiO_2/Al_2O_3 ratio of 1.38) and M2 (metakaolin with SiO_2/Al_2O_3 ratio of 1.41) subjected to different temperatures (a) ^{25}M1, (b) ^{1,400}M1, (c) ^{25}M1$_{1.57}$, (d) ^{1,400}M1$_{1.57}$, (e) ^{25}M2, (f) ^{1,400}M2, (g) ^{25}M2$_{1.57}$, and (h) ^{1,400}M2$_{1.57}$ samples [121]

Recently, Tiffo et al. [130] produced AACs from the combination of kaolin mixed with aluminum oxide up to 30 wt%. When exposed to high temperatures in the range of 300-1,200 °C, the samples containing 10% aluminum oxide heated at 1,150 °C developed a compressive strength of 65 MPa. The improvement in the performance recorded at this temperature is related to the formation of crystalline phases like mullite, corundum, and nepheline leading to their contribution to form Al-Si minerals. Vidal et al. [121] varied the ammonium molybdate content on two metakaolin-

based AACs and then subjected the AACs to 1,400 °C. From SEM analysis presented in Figure 9, they observed that the incorporation of ammonium molybdate induced some changes in phases at high temperatures. The micrographs of end binders appear dense and vitreous with homogeneous structure leading to the formation of interconnected pores within the matrixes. This densification is well pronounced when incorporating 1.57 wt% of ammonium molybdate resulting in good distribution between the binder phase and other components in the matrix.

Elimbi et al. [123] observed a decrease in the halo peak 2-theta range from XRD analysis due to the appearance of reflection peaks of crystalline phases when the temperature of metakaolin-based AACs was increased from 25 to 1,000 °C. This reduction in halo peak on XRD indicates the formed amorphous phase after polymerization justifying the reduction in the mechanical strength that was observed in the AACs studied. However, a reverse effect was noticed by Barbosa and Mackenzie [131] who did not record any reduction in amorphous content the metakaolin used as a precursor in AACs was replaced up to 20 wt% by various inorganic fillers. After heating the AACs to 900 °C, the X-ray patterns of the AACs were almost similar in terms of developed halo peak 2 theta range and the only reduction peaks were that of the quartz mineral. A similar trend has been observed by the findings of Tchakoute et al. [127] where the waste glass or rice husk ash (RHA) with NaOH as activators to produce the metakaolin-based AACs. After heating the resulting AACs to 800 °C, no reflection peak of the new phase was observed on the diffractograms. The halo peak appearing on each diffractogram not changing with increasing temperature indicates the stability of the synthesized AAC products. This observation was also complimented by similar compressive strength observed in heated between 400 and 600 °C.

Nobouassia Bewa et al. [132] identified the newly formed mineralogical phases such as phospho-tridymite and phospho-cristobalite from XRD diffractograms of heated acid consolidated metakaolin-based AACs between 200 and 1,000 °C. The presence of these new crystalline phases is linked to the polymorphic transition of berlinite according to these authors. Duan et al. [117] evaluated the thermal stability of AACs made from combined metakaolin and fly ash in a 1/1 weight ratio up to 1,000 °C. Findings from the study showed that increasing the heating temperature from 20 to 400 °C resulted in an increase in compressive strength from 35 to 39 and 59 to 72 MPa for AACs cured for 3 and 28 days, respectively. However, when applying a heating temperature above 400 °C, a reduction in the mechanical performance was observed. Nana et al. [104] replaced metakaolin with 70, 75, 80, and 85 wt% of pegmatite and investigated the thermal of the resulting geopolymer composite products from 25 to 1,100 °C. From their study incorporating pegmatite was a benefit for the stability of matrices that achieved high strength in the range of 800-1,000 °C linking to lower porosity.

3. Conclusions

The purpose of this paper is to review alkali-activated clay composite materials that use kaolinitic clays as an additive in various dosages or as a composite material precursor. Calcined clays have been added to lower the cost of calcination while improving certain semi-crystalline materials with low reactive phases. Therefore, the present paper explores and discusses the fresh (workability, setting time) and hardening (compressive and flexural strength) as well as microstructural properties of AACs prepared from clay materials as main solid precursors or secondary source materials used for the synthesis of AACs. Discussions presented in the paper showed that various clay materials such as metakaolin, metahalloysite, feldspar, slag, fly ash, silica, and laterite can be used to produce AACs for various construction applications. It was also found that various clay materials can be incorporated alongside other precursors as a binary or ternary precursor to complement the performance of AACs. However, the resulting performance of composites incorporating clay materials is dependent on the properties and treatments of the clay materials. Thus, calcined clay with a high amount of reactive phase highly improved the end properties of AACs. While other factors impacting the physical properties were the liquid-to-solid ratio of alkaline activators, curing regime, and molarity of alkaline activators in terms of silica modulus.

For solid precursors with low reactivity, such as pegmatite, a small amount of calcined clay is required to achieve high performance. Mechanical activation was used to improve its reactivity by enhancing the physicochemical properties required for the formation of more binder phases.

As there are limited studies, especially in terms of durability performance on clay-based AACs, it is recommended

that more research and development should be carried out in this area. The critical durability performance of clay-based AACs is in terms of the resistance of the composites to freeze-thaw cycles, dry-wet cycles, and severe environments such as acid and alkali. It is also imminent to carry out a comprehensive life cycle assessment of clay-based AACs in order to accurately quantify their sustainability and economic benefits.

Funding

The author of the manuscript did not receive any funding or grants for this research.

Conflicts of interest

The author declares no competing financial interest.

References

[1] A. Buchwald, C. Kaps, and M. Hohmann, "Alkali-activated binders and pozzolan cement binders-complete binder reaction or two sides of the same story," Proceedings of the 11th International Congress on the Chemistry of Cement (ICCC), Durban, South Africa, 2003.
[2] C. J. Shi, D. Roy, and P. Krivenko, *Alkali-Activated Cements and Concretes*. London: CRC press, 2003.
[3] J. Davidovits, "Geopolymers: inorganic polymeric new materials," *Journal of Thermal Analysis and Calorimetry*, vol. 37, no. 8, pp. 1633-1656, 1991.
[4] P. Duxson, J. L. Provis, G. C. Lukey, F. Separovic, and J. S. J. van Deventer, "29Si NMR study of structural ordering in aluminosilicate geopolymer gels," *Langmuir*, vol. 21, no. 7, pp. 3028-3036, 2005.
[5] H. Rahier, W. Simons, B. Van Mele, and M. Biesemans, "Low-temperature synthesized aluminosilicate glasses: Part III Influence of the composition of the silicate solution on production, structure and properties," *Journal of Materials Science*, vol. 32, pp. 2237-2247, 1997.
[6] A. Naghizadeh, S. O. Ekolu, and F. Solomon, "Challenges and problems of geopolymer brick masonry: A review," *Key Engineering Materials*, vol. 916, pp. 136-144, 2022.
[7] B. Kim and S. Lee, "Review on characteristics of metakaolin-based geopolymer and fast setting," *Journal of the Korean Ceramic Society*, vol. 57, no. 4, pp. 368-377, 2020.
[8] A. Adesina, J. Cercel, and S. Das, "Effect of curing conditions on the compressive strength of sodium carbonate activated slag-glass powder mortar," *Canadian Journal of Civil Engineering*, vol. 48, no. 8, pp. 1056-1061, 2020.
[9] A. Naghizadeh and S. Ekolu, "Effect of different mixture parameters on the setting time of fly ash/rice husk ash-based geopolymer mortar," MATEC Web of Conferences, Hulis, France: EDP Sciences, 2022, pp. 05001. https://doi.org/10.1051/matecconf/202236105001
[10] A. Naghizadeh and S. O. Ekolu, "Effects of compositional and physico-chemical mix design parameters on properties of fly ash geopolymer mortars," Silicon, vol. 13, no. 12, pp. 4669-4680, 2021.
[11] B. Akturk, M. Abolfathi, S. Ulukaya, A. B. Kizilkanat, T. J. N. Hooper, L. Gu, E. H. Yang, and C. Unluer, "Hydration kinetics and performance of sodium carbonate-activated slag-based systems containing reactive MgO and metakaolin under carbonation," Cement and Concrete Composites, vol. 132, pp. 104617, 2022.
[12] L. F. Fan, D. K. Chen, and W. L. Zhong, "Effects of slag and alkaline solution contents on bonding strength of geopolymer-concrete composites," Construction and Building Materials, vol. 406, pp. 133391, 2023.
[13] S. Oyebisi, F. Olutoge, P. Kathirvel, I. Oyaotuderekumor, D. Lawanson, J. Nwani, A. Ede, and R. Kaze, "Sustainability assessment of geopolymer concrete synthesized by slag and corncob ash," Case Studies in Construction Materials, vol. 17, pp. e01665, 2022.
[14] S. K. Das, J. Mishra, S. M. Mustakim, A. Adesina, C. R. Kaze, and D. Das, "Sustainable utilization of ultrafine rice husk ash in alkali activated concrete: Characterization and performance evaluation," Journal of Sustainable Cement-Based Materials, vol. 11, no. 2, pp. 100-112, 2022.
[15] C. R. Kaze, A. Adesina, G. L. Lecomte-Nana, J. V. S. Metekong, L. V. E. K. Samen, E. Kamseu, and U. C. Melo, "Synergetic effect of rice husk ash and quartz sand on microstructural and physical properties of laterite clay based

geopolymer," Journal of Building Engineering, vol. 43, pp. 103229, 2021.
[16] C. R. Kaze, A. Naghizadeh, L. Tchadjie, A. Adesina, J. N. Y. Djobo, J. G. D. Nemaleu, E. Kamseu, U. C. Melo, and B. A. Tayeh, "Lateritic soils based geopolymer materials: A review," Construction and Building Materials, vol. 344, pp. 128157, 2022.
[17] C. R. Kaze, L. M. B. à Moungam, J. V. S. Metekong, T. S. Alomayri, A. Naghizadeh, and L. Tchadjie, "Thermal behaviour, microstructural changes and mechanical properties of alkali-activated volcanic scoria-fired waste clay brick blends," Developments in the Built Environment, vol. 14, pp. 100153, 2023.
[18] M. Uysal, Y. Aygörmez, O. Canpolat, T. Cosgun, and Ö. F. Kuranlı, "Investigation of using waste marble powder, brick powder, ceramic powder, glass powder, and rice husk ash as eco-friendly aggregate in sustainable red mud-metakaolin based geopolymer composites," Construction and Building Materials, vol. 361, pp. 129718, 2022.
[19] J. V. S. Metekong, C. R. Kaze, J. G. Deutou, P. Venyite, A. Nana, E. Kamseu, U. C. Melo, and T. T. Tatietse, "Evaluation of performances of volcanic-ash-laterite based blended geopolymer concretes: Mechanical properties and durability," Journal of Building Engineering, vol. 34, pp. 101935, 2021.
[20] L. M. B. à Moungam, K. V. Tchieda, H. Mohamed, N. C. Pecheu, R. C. Kaze, E. Kamseu, A. D. Mvondo-Ze, and I. K. Tonle, "Efficiency of volcanic ash-based porous geopolymers for the removal of Pb^{2+}, Cd^{2+} and Hg^{2+} from aqueous solution," Cleaner Materials, vol. 5, pp. 100106, 2022.
[21] A. S. Albidah, "Effect of partial replacement of geopolymer binder materials on the fresh and mechanical properties: A review," Ceramics International, vol. 47, no. 11, pp. 14923-14943, 2021.
[22] M. Muraleedharan and Y. Nadir, "Factors affecting the mechanical properties and microstructure of geopolymers from red mud and granite waste powder: A review," Ceramics International, vol. 47, no. 10, pp. 13257-13279, 2021.
[23] W. Song, T. Guo, P. Han, X. Wang, F. Ma, and B. He, "Durability study and mechanism analysis of red mud-coal metakaolin geopolymer concrete under a sulfate environment," Construction and Building Materials, vol. 409, pp. 133990, 2023.
[24] T. M. Tognonvi, A. B. Pascual, and A. Tagnit-Hamou, "Physico-chemistry of geopolymers based on recycled glass powder and metakaolin: Effect of metakaolin content," Materials Today: Proceedings, vol. 58, pp. 1508-1514, 2022.
[25] A. Adesina, "Performance and sustainability overview of sodium carbonate activated slag materials cured at ambient temperature," Resources, Environment and Sustainability, vol. 3, pp. 100016, 2021.
[26] V. Bilek, O. Sucharda, and D. Bujdos, "Frost resistance of alkali-activated concrete-an important pillar of their sustainability," Sustainability, vol. 13, no. 2, pp. 473, 2021.
[27] J. G. D. Nemaleu, C. R. Kaze, J. V. S. Metekong, A. Adesina, T. Alomayri, M. Stuer, and E. Kamseu, "Synthesis and characterization of eco-friendly mortars made with RHA-NaOH activated fly ash as binder at room temperature," Cleaner Materials, vol. 1, pp. 100010, 2021.
[28] S. Marathe, I. R. Mithanthaya, and R. Y. Shenoy, "Durability and microstructure studies on Slag-Fly Ash-Glass powder based alkali activated pavement quality concrete mixes," Construction and Building Materials, vol. 287, pp. 123047, 2021.
[29] B. B. Jindal, T. Alomayri, A. Hasan, and C. R. Kaze, "Geopolymer concrete with metakaolin for sustainability: a comprehensive review on raw material's properties, synthesis, performance, and potential application," Environmental Science and Pollution Research, vol. 30, no. 10, pp. 25299-25324, 2023.
[30] C. R. Kaze, S. B. K. Jiofack, Ö. Cengiz, T. S. Alomayri, A. Adesina, and H. Rahier, "Reactivity and mechanical performance of geopolymer binders from metakaolin/meta-halloysite blends," Construction and Building Materials, vol. 336, pp. 127546, 2022.
[31] C. R. Kaze, G. L. Lecomte-Nana, E. Kamseu, P. S. Camacho, J. L. Provis, M. Duttine, A. Wattiaux, and U. C. Melo, "Mechanical and physical properties of inorganic polymer cement made of iron-rich laterite and lateritic clay: A comparative study," Cement and Concrete Research, vol. 140, pp. 106320, 2021.
[32] K. Chen, D. Wu, M. Yi, Q. Cai, and Z. Zhang, "Mechanical and durability properties of metakaolin blended with slag geopolymer mortars used for pavement repair," Construction and Building Materials, vol. 281, pp. 122566, 2021.
[33] G. GÖRhan and G. KÜRklÜ, "Investigation of the effect of metakaolin substitution on physicomechanical properties of fly ash-based geopolymer mortars," Materials Today: Proceedings, vol. 81, pp. 35-42, 2023.
[34] C. R. Kaze, T. Alomayri, A. Hasan, S. Tome, G. L. Lecomte-Nana, J. G. D. Nemaleu, H. K. Tchakoute, E. Kamseu, U. C. Melo, and H. Rahier, "Reaction kinetics and rheological behaviour of meta-halloysite based geopolymer cured at room temperature: Effect of thermal activation on physicochemical and microstructural properties,"

Applied Clay Science, vol. 196, pp. 105773, 2020.
[35] A. Elimbi, H. K. Tchakoute, and D. Njopwouo, "Effects of calcination temperature of kaolinite clays on the properties of geopolymer cements," Construction and Building Materials, vol. 25, no. 6, pp. 2805-2812, 2011.
[36] G. Wang, S. Chen, M. Xia, W. Zhong, X. Han, B. Luo, M. M. S. Sabri, and J. Huang, "Experimental study on durability degradation of geopolymer-stabilized soil under sulfate erosion," Materials, vol. 15, no. 15, pp. 5114, 2022.
[37] Y. Su, B. Luo, Z. Luo, F. Xu, H. Huang, Z. Long, and C. Shen, "Mechanical characteristics and solidification mechanism of slag/fly ash-based geopolymer and cement solidified organic clay: A comparative study," Journal of Building Engineering, vol. 71, pp. 106459, 2023.
[38] J. Ayawanna and A. Poowancum, "Enhancing flexural strength of metakaolin-based geopolymer reinforced with different types of fibers," Sustainable Chemistry and Pharmacy, vol. 37, pp. 101439, 2024.
[39] A. C. Constâncio Trindade, K. Sankar, F. de Andrade Silva, and W. M. Kriven, "Fabrication and mechanical properties of metakaolin-based geopolymer composites reinforced with auxetic fabrics," Journal of the American Ceramic Society, vol. 106, no. 8, pp. 4852-4862, 2023.
[40] M. Zhang, H. Xu, A. L. P. Zeze, and J. Zhang, "Metakaolin-based geopolymer composites modified by epoxy resin and silane: Mechanical properties and organic-inorganic interaction mechanism," Applied Clay Science, vol. 232, pp. 106767, 2023.
[41] H. Wang, C. Li, Z. Peng, and S. Zhang, "Characterization and thermal behavior of kaolin," Journal of Thermal Analysis and Calorimetry, vol. 105, no. 1, pp. 157-160, 2011.
[42] C. Belver, M. A. Bañares, and M. A. Vicente, "Preparation of porous silica by acid activation of metakaolins," Studies in Surface Science and Catalysis, vol. 144, pp. 307-314, 2002.
[43] Y. M. Liew, H. Kamarudin, A. M. M. Al Bakri, M. Luqman, I. K. Nizar, C. M. Ruzaidi, and C. Y. Heah, "Processing and characterization of calcined kaolin cement powder," Construction and Building Materials, vol. 30, pp. 794-802, 2012.
[44] P. Duan, C. Yan, and W. Zhou, "Influence of partial replacement of fly ash by metakaolin on mechanical properties and microstructure of fly ash geopolymer paste exposed to sulfate attack," Ceramics International, vol. 42, no. 2, pp. 3504-3517, 2016.
[45] H. Alanazi, J. Hu, and Y. R. Kim, "Effect of slag, silica fume, and metakaolin on properties and performance of alkali-activated fly ash cured at ambient temperature," Construction and Building Materials, vol. 197, pp. 747-756, 2019.
[46] A. G. Borçato, M. Thiesen, and R. A. Medeiros-Junior, "Mechanical properties of metakaolin-based geopolymers modified with different contents of quarry dust waste," Construction and Building Materials, vol. 400, pp. 132854, 2023.
[47] M. Amin, Y. Elsakhawy, K. Abu el-hassan, and B. A. Abdelsalam, "Behavior evaluation of sustainable high strength geopolymer concrete based on fly ash, metakaolin, and slag," Case Studies in Construction Materials, vol. 16, pp. e00976, 2022.
[48] M. Li, R. Luo, L. Qin, H. Liu, P. Duan, W. Jing, Z. Zhang, and X. Liu, "High temperature properties of graphene oxide modified metakaolin based geopolymer paste," Cement and Concrete Composites, vol. 125, pp. 104318, 2022.
[49] N. Bheel, P. Awoyera, T. Tafsirojjaman, and N. H. Sor, "Synergic effect of metakaolin and groundnut shell ash on the behavior of fly ash-based self-compacting geopolymer concrete," Construction and Building Materials, vol. 311, pp. 125327, 2021.
[50] C. K. Gautam and P. Alam, "To study the effect of geopolymer concrete by using metakaolin & bottom ash," Materials Today: Proceedings, vol. 74, pp. 1028-1034, 2023.
[51] C. Jithendra, V. N. Dalawai, and S. Elavenil, "Effects of metakaolin and sodium silicate solution on workability and compressive strength of sustainable Geopolymer mortar," Materials Today: Proceedings, vol. 51, pp. 1580-1584, 2022.
[52] H. Peng, C. Cui, Z. Liu, C. S. Cai, and Y. Liu, "Synthesis and reaction mechanism of an alkali-activated metakaolin-slag composite system at room temperature," Journal of Materials in Civil Engineering, vol. 31, no. 1, pp. 04018345, 2019.
[53] A. Driouich, S. A. El Hassani, N. H. Sor, Z. Zmirli, S. El harfaoui, M. A. Othuman Mydin, A. Aziz, A. Farouk Deifalla, and H. Chaair, "Mix design optimization of metakaolin-slag-based geopolymer concrete synthesis using RSM," Results in Engineering, vol. 20, pp. 101573, 2023.
[54] N. Ranjbar, C. Kuenzel, C. Gundlach, P. Kempen, and M. Mehrali, "Halloysite reinforced 3D-printable

geopolymers," Cement and Concrete Composites, vol. 136, pp. 104894, 2023.
[55] A. Hasnaoui, A. Bourguiba, N. Sebaibi, and M. Boutouil, "Valorization of queen scallop shells in the preparation of metakaolin-based geopolymer mortars," Journal of Building Engineering, vol. 53, pp. 104578, 2022.
[56] M. B. Jaji, G. P. A. G. van Zijl, and A. J. Babafemi, "Slag-modified metakaolin-based 3D printed geopolymer: Mechanical characterisation, microstructural properties, and nitrogen physisorption pore analysis," Journal of Building Engineering, vol. 81, pp. 108166, 2024.
[57] M. B. Jaji, G. P. A. G. van Zijl, and A. J. Babafemi, "Slag-modified metakaolin-based geopolymer for 3D concrete printing application: Evaluating fresh and hardened properties," Cleaner Engineering and Technology, vol. 15, pp. 100665, 2023.
[58] J. N. Y. Djobo and D. Stephan, "The reaction of calcium during the formation of metakaolin phosphate geopolymer binder," Cement and Concrete Research, vol. 158, pp. 106840, 2022.
[59] J. G. D. Nemaleu, R. C. Kaze, S. Tome, T. Alomayri, H. Assaedi, E. Kamseu, U. C. Melo, and V. M. Sglavo, "Powdered banana peel in calcined halloysite replacement on the setting times and engineering properties on the geopolymer binders," Construction and Building Materials, vol. 279, pp. 122480, 2021.
[60] H. Guo, B. Zhang, L. Deng, P. Yuan, M. Li, and Q. Wang, "Preparation of high-performance silico-aluminophosphate geopolymers using fly ash and metakaolin as raw materials," Applied Clay Science, vol. 204, pp. 106019, 2021.
[61] J. G. D. Nemaleu, E. A. Belela, A. Nana, R. C. Kaze, P. Venyite, R. N. Yanou, J. N. Y. Djobo, and E. Kamseu, "Feasibilty of valorizing quarry wastes in the synthesis of geopolymer binders: engineering performances and microstructure," Environmental Science and Pollution Research, vol. 29, no. 33, pp. 50804-50818, 2022.
[62] R. B. E. Boum, C. R. Kaze, J. G. D. Nemaleu, V. B. Djaoyang, N. Y. Rachel, P. L. Ninla, F. M. Owono, and E. Kamseu, "Thermal behaviour of metakaolin-bauxite blends geopolymer: microstructure and mechanical properties," SN Applied Sciences, vol. 2, no. 8, pp. 1358, 2020.
[63] B. N. Bayiha, N. Billong, E. Yamb, R. C. Kaze, and R. Nzengwa, "Effect of limestone dosages on some properties of geopolymer from thermally activated halloysite," Construction and Building Materials, vol. 217, pp. 28-35, 2019.
[64] B. Zhang, P. Yuan, H. Guo, L. Deng, Y. Li, L. Li, Q. Wang, and D. Liu, "Effect of curing conditions on the microstructure and mechanical performance of geopolymers derived from nanosized tubular halloysite," Construction and Building Materials, vol. 268, pp. 121186, 2021.
[65] C. R. Kaze, P. Venyite, A. Nana, D. N. Juvenal, H. K. Tchakoute, H. Rahier, E. Kamseu, U. C. Melo, and C. Leonelli, "Meta-halloysite to improve compactness in iron-rich laterite-based alkali activated materials," Materials Chemistry and Physics, vol. 239, pp. 122268, 2020.
[66] T. Yu, B. Zhang, P. Yuan, H. Guo, D. Liu, J. Chen, H. Liu, and L. S. Belaroui, "Optimization of mechanical performance of limestone calcined clay cement: Effects of calcination temperature of nanosized tubular halloysite, gypsum content, and water/binder ratio," Construction and Building Materials, vol. 389, pp. 131709, 2023.
[67] S. Zhou, Z. Yang, R. Zhang, and F. Li, "Preparation, characterization and rheological analysis of eco-friendly road geopolymer grouting materials based on volcanic ash and metakaolin," Journal of Cleaner Production, vol. 312, pp. 127822, 2021.
[68] K. W. Lo, K. L. Lin, T. W. Cheng, Y. M. Chang, and J. Y. Lan, "Effect of nano-SiO_2 on the alkali-activated characteristics of spent catalyst metakaolin-based geopolymers," Construction and Building Materials, vol. 143, pp. 455-463, 2017.
[69] J. N. Y. Djobo, L. N. Tchadjié, H. K. Tchakoute, B. B. D. Kenne, A. Elimbi, and D. Njopwouo, "Synthesis of geopolymer composites from a mixture of volcanic scoria and metakaolin," Journal of Asian Ceramic Societies, vol. 2, no. 4, pp. 387-398, 2014.
[70] K. Gao, K. L. Lin, D. Y. Wang, C. L. Hwang, H. S. Shiu, Y. M. Chang, and T. W. Cheng, "Effects SiO_2/Na_2O molar ratio on mechanical properties and the microstructure of nano-SiO_2 metakaolin-based geopolymers," Construction and Building Materials, vol. 53, pp. 503-510, 2014.
[71] Z. Zidi, M. Ltifi, and I. Zafar, "Synthesis and attributes of nano-SiO_2 local metakaolin based-geopolymer," Journal of Building Engineering, vol. 33, pp. 101586, 2021.
[72] H. T. Kouamo, A. Elimbi, J. A. Mbey, C. J. N. Sabouang, and D. Njopwouo, "The effect of adding alumina-oxide to metakaolin and volcanic ash on geopolymer products: A comparative study," Construction and Building Materials, vol. 35, pp. 960-969, 2012.
[73] R. Rajamma, J. A. Labrincha, and V. M. Ferreira, "Alkali activation of biomass fly ash-metakaolin blends," Fuel, vol. 98, pp. 265-271, 2012.

[74] K. Zulkifly, H. Cheng-Yong, L. Yun-Ming, M. M. A. B. Abdullah, O. Shee-Ween, and M. S. B. Khalid, "Effect of phosphate addition on room-temperature-cured fly ash-metakaolin blend geopolymers," Construction and Building Materials, vol. 270, pp. 121486, 2020.
[75] J. Liu, X. Li, Y. Lu, and X. Bai, "Effects of Na/Al ratio on mechanical properties and microstructure of red mud-coal metakaolin geopolymer," Construction and Building Materials, vol. 263, pp. 120653, 2020.
[76] P. N. Lemougna, K. J. D. MacKenzie, and U. F. C. Melo, "Synthesis and thermal properties of inorganic polymers (geopolymers) for structural and refractory applications from volcanic ash," Ceramics International, vol. 37, no. 8, pp. 3011-3018, 2011.
[77] H. K. Tchakoute, A. Elimbi, E. Yanne, and C. N. Djangang, "Utilization of volcanic ashes for the production of geopolymers cured at ambient temperature," Cement and Concrete Composites, vol. 38, pp. 75-81, 2013.
[78] A. Nana, E. N. Sakue, P. Venyite, S. C. D. Anensong, N. Epey, A. A. Adediran, E. Kamseu, S. Kumar, and C. Leonelli, "Effect of milled pegmatite quarry wastes powders on structure, microstructure and mechanical properties of pegmatite-based geopolymers," Materialia, vol. 33, pp. 102022, 2024.
[79] C. R. Kaze, P. N. Lemougna, T. Alomayri, H. Assaedi, A. Adesina, S. K. Das, G. L. Lecomte-Nana, E. Kamseu, U. C. Melo, and C. Leonelli, "Characterization and performance evaluation of laterite based geopolymer binder cured at different temperatures," Construction and Building Materials, vol. 270, pp. 121443, 2021.
[80] H. Zhu, G. Liang, H. Li, Q. Wu, C. Zhang, Z. Yin, and S. Hua, "Insights to the sulfate resistance and microstructures of alkali-activated metakaolin/slag pastes," Applied Clay Science, vol. 202, pp. 105968, 2021.
[81] L. Kuang, G. Li, J. Xiang, W. Ma, and X. Cui, "Effect of seawater on the properties and microstructure of metakaolin/slag-based geopolymers," Construction and Building Materials, vol. 397, pp. 132418, 2023.
[82] M. Li, H. Liu, P. Duan, S. Ruan, Z. Zhang, and W. Ge, "The effects of lithium slag on microstructure and mechanical performance of metakaolin-based geopolymers designed by response surface method (RSM)," Construction and Building Materials, vol. 299, pp. 123950, 2021.
[83] H. Güllü and A. A. Agha, "The rheological, fresh and strength effects of cold-bonded geopolymer made with metakaolin and slag for grouting," Construction and Building Materials, vol. 274, pp. 122091, 2021.
[84] M. B. Kretzer, C. Effting, S. Schwaab, and A. Schackow, "Hybrid geopolymer-cement coating mortar optimized based on metakaolin, fly ash, and granulated blast furnace slag," Cleaner Engineering and Technology, vol. 4, pp. 100153, 2021.
[85] M. Su, Q. Zhong, and H. Peng, "Regularized multivariate polynomial regression analysis of the compressive strength of slag-metakaolin geopolymer pastes based on experimental data," Construction and Building Materials, vol. 303, pp. 124529, 2021.
[86] P. Zhang, K. Wang, J. Wang, J. Guo, and Y. Ling, "Macroscopic and microscopic analyses on mechanical performance of metakaolin/fly ash based geopolymer mortar," Journal of Cleaner Production, vol. 294, pp. 126193, 2021.
[87] P. Zhang, X. Han, S. Hu, J. Wang, and T. Wang, "High-temperature behavior of polyvinyl alcohol fiber-reinforced metakaolin/fly ash-based geopolymer mortar," Composites Part B: Engineering, vol. 244, pp. 110171, 2022.
[88] Q. Zhang, D. Huang, X. Zhang, L. Lin, Z. Wang, W. Tang, and X. Qiang, "Improving the properties of metakaolin/fly ash composite geopolymers with ultrafine fly ash ground by steam-jet mill," Construction and Building Materials, vol. 387, pp. 131673, 2023.
[89] E. Kamseu, A. T. Akono, A. Nana, R. C. Kaze, and C. Leonelli, "Performance of geopolymer composites made with feldspathic solid solutions: Micromechanics and microstructure," Cement and Concrete Composites, vol. 124, pp. 104241, 2021.
[90] J. C. Soares, J. S. de Azevedo, and D. P. Dias, "Effect of temperature on metakaolin-quartz powder geopolymer binder with different combinations of silicates and hydroxides," Case Studies in Construction Materials, vol. 16, pp. e00813, 2022.
[91] H. M. Khater and M. Gharieb, "Synergetic effect of nano-silica fume for enhancing physico-mechanical properties and thermal behavior of MK-geopolymer composites," Construction and Building Materials, vol. 350, pp. 128879, 2022.
[92] A. Nana, N. Epey, K. C. Rodrique, J. G. N. Deutou, J. N. Y. Djobo, S. Tomé, T. S. Alomayri, J. Ngouné, E. Kamseu, and C. Leonelli, "Mechanical strength and microstructure of metakaolin/volcanic ash-based geopolymer composites reinforced with reactive silica from rice husk ash (RHA)," Materialia, vol. 16, pp. 101083, 2021.
[93] N. F. J. Nadia, A. Gharzouni, B. Nait-Ali, L. Ouamara, I. M. Ndassa, G. Bebga, K. Elie, and S. Rossignol, "Comparative study of laterite and metakaolin/hematite-based geopolymers: Effect of iron source and alkalization," Applied Clay Science, vol. 233, pp. 106824, 2023.

[94] X. Han, P. Zhang, Y. Zheng, and J. Wang, "Utilization of municipal solid waste incineration fly ash with coal fly ash/metakaolin for geopolymer composites preparation," Construction and Building Materials, vol. 403, pp. 133060, 2023.
[95] P. Venyite, E. C. Makone, R. C. Kaze, A. Nana, J. G. D. Nemaleu, E. Kamseu, U. C. Melo, and C. Leonelli, "Effect of combined metakaolin and basalt powder additions to laterite-based geopolymers activated by Rice Husk Ash (RHA)/NaOH solution," Silicon, vol. 14, no. 4, pp. 1643-1662, 2022.
[96] F. A. Shilar, S. V. Ganachari, V. B. Patil, and K. S. Nisar, "Evaluation of structural performances of metakaolin based geopolymer concrete," Journal of Materials Research and Technology, vol. 20, pp. 3208-3228, 2022.
[97] X. Tian, K. Liu, X. Yang, T. Jiang, B. Chen, Z. Tian, J. Wu, L. Xia, D. Huang, and H. Peng, "Synthesis of metakaolin-based geopolymer foamed materials using municipal solid waste incineration fly ash as a foaming agent," Waste Management, vol. 169, pp. 101-111, 2023.
[98] J. Liu, L. Hu, L. Tang, and J. Ren, "Utilisation of municipal solid waste incinerator (MSWI) fly ash with metakaolin for preparation of alkali-activated cementitious material," Journal of Hazardous Materials, vol. 402, pp. 123451, 2021.
[99] P. N. Lemougna, K. Wang, Q. Tang, E. Kamseu, N. Billong, U. C. Melo, and X. Cui, "Effect of slag and calcium carbonate addition on the development of geopolymer from indurated laterite," Applied Clay Science, vol. 148, pp. 109-117, 2017.
[100] J. G. N. Deutou, R. C. Kaze, E. Kamseu, and V. M. Sglavo, "Controlling the thermal stability of kyanite-based refractory geopolymers," Materials, vol. 14, no. 11, pp. 2903, 2021.
[101] A. Nana, E. Kamseu, A. T. Akono, J. Ngouné, J. N. Y. Djobo, H. K. Tchakoute, M. C. Bignozzi, and C. Leonelli, "Particles size and distribution on the improvement of the mechanical performance of high strength solid solution based inorganic polymer composites: A microstructural approach," Materials Chemistry and Physics, vol. 267, pp. 124602, 2021.
[102] E. Kamseu, M. Cannio, E. A. Obonyo, F. Tobias, M. C. Bignozzi, V. M. Sglavo, and C. Leonelli, "Metakaolin-based inorganic polymer composite: Effects of fine aggregate composition and structure on porosity evolution, microstructure and mechanical properties," Cement and Concrete Composites, vol. 53, pp. 258-269, 2014.
[103] E. Kamseu, M. C. Bignozzi, U. C. Melo, C. Leonelli, and V. M. Sglavo, "Design of inorganic polymer cements: Effects of matrix strengthening on microstructure," Construction and Building Materials, vol. 38, pp. 1135-1145, 2013.
[104] A. Nana, R. C. Kaze, T. S. Alomayri, H. S. Assaedi, J. G. N. Deutou, J. Ngoune, H. K. Tchakoute, E. Kamseu, and C. Leonelli, "Innovative porous ceramic matrices from inorganic polymer composites (IPCs): Microstructure and mechanical properties," Construction and Building Materials, vol. 273, pp. 122032, 2021.
[105] A. Nana, T. Alomayri, S. Tome, S. Nath, E. Kamseu, M. C. Bignozzi, C. Leonelli, and S. Kumar, "Reaction kinetics and microstructure of pegmatite-based geopolymer composites: influence of calcined clay nature," Journal of the American Ceramic Society, vol. 107, no. 4, pp. 2693-2708, 2024.
[106] K. Gao, K. L. Lin, D. Y. Wang, C. L. Hwang, B. L. A. Tuan, H. S. Shiu, and T. W. Cheng, "Effect of nano-SiO_2 on the alkali-activated characteristics of metakaolin-based geopolymers," Construction and Building Materials, vol. 48, pp. 441-447, 2013.
[107] H. Cheng, K. L. Lin, R. Cui, C. L. Hwang, Y. M. Chang, and T. W. Cheng, "The effects of SiO_2/Na_2O molar ratio on the characteristics of alkali-activated waste catalyst-metakaolin based geopolymers," Construction and Building Materials, vol. 95, pp. 710-720, 2015.
[108] A. Buchwald, M. Vicent, R. Kriegel, C. Kaps, M. Monzó, and A. Barba, "Geopolymeric binders with different fine fillers-Phase transformations at high temperatures," Applied Clay Science, vol. 46, no. 2, pp. 190-195, 2009.
[109] M. C. Bignozzi, S. Manzi, I. Lancellotti, E. Kamseu, L. Barbieri, and C. Leonelli, "Mix-design and characterization of alkali activated materials based on metakaolin and ladle slag," Applied Clay Science, vol. 73, pp. 78-85, 2013.
[110] R. Belinga Essama Boum, F. Mvondo Owono, C. R. Kaze, J. C. Essomba Essomba, "Thermal behavior of acidic and alkali activated laterite based geopolymer: a comparative study," Geosystem Engineering, vol. 25, no. 5-6, pp. 225-238, 2022.
[111] A. Nana, G. Ridolfi, C. S. D. Anensong, S. B. L. Ngomade, A. A. Adediran, J. Ngouné, E. Kamseu, S. Kumar, M. C. Bignozzi, and C. Leonelli, "Thermal, mechanical, and microstructural properties of inorganic polymer composites from quarry wastes (feldspathic minerals)," Journal of Thermal Analysis and Calorimetry, vol. 148, no. 19, pp. 10021-10035, 2023.
[112] C. R. Kaze, A. Nana, G. L. Lecomte-Nana, J. G. N. Deutou, E. Kamseu, U. C. Melo, F. Andreola, and C. Leonelli, "Thermal behaviour and microstructural evolution of metakaolin and meta-halloysite-based geopolymer binders: a

comparative study," Journal of Thermal Analysis and Calorimetry, vol. 147, no. 3, pp. 2055-2071, 2022.
[113]J. G. D. Nemaleu, V. Bakaine Djaoyang, A. Bilkissou, C. R. Kaze, R. B. E. Boum, J. N. Y. Djobo, P. L. Ninla, and E. Kamseu, "Investigation of groundnut shell powder on development of lightweight metakaolin based geopolymer composite: Mechanical and microstructural properties," Silicon, vol. 14, no. 2, pp. 449-461, 2022.
[114]S. M. A. Qaidi, D. S. Atrushi, A. S. Mohammed, H. U. Ahmed, R. H. Faraj, W. Emad, B. A. Tayeh, and H. M. Najm, "Ultra-high-performance geopolymer concrete: A review," Construction and Building Materials, vol. 346, pp. 128495, 2022.
[115]C. Fu, H. Ye, K. Zhu, D. Fang, and J. Zhou, "Alkali cation effects on chloride binding of alkali-activated fly ash and metakaolin geopolymers," Cement and Concrete Composites, vol. 114, pp. 103721, 2020.
[116]M. Jin, Z. Zheng, Y. Sun, L. Chen, and Z. Jin, "Resistance of metakaolin-MSWI fly ash based geopolymer to acid and alkaline environments," Journal of Non-Crystalline Solids, vol. 450, pp. 116-122, 2016.
[117]P. Duan, C. Yan, W. Zhou, W. Luo, and C. Shen, "An investigation of the microstructure and durability of a fluidized bed fly ash-metakaolin geopolymer after heat and acid exposure," Materials & Design, vol. 74, pp. 125-137, 2015.
[118]F. Matalkah, T. Salem, M. Shaafaey, and P. Soroushian, "Drying shrinkage of alkali activated binders cured at room temperature," Construction and Building Materials, vol. 201, pp. 563-570, 2019.
[119]A. Mobili, A. Belli, C. Giosuè, T. Bellezze, and F. Tittarelli, "Metakaolin and fly ash alkali-activated mortars compared with cementitious mortars at the same strength class," Cement and Concrete Research, vol. 88, pp. 198-210, 2016.
[120]B. J. Frasson and J. C. Rocha, "Drying shrinkage behavior of geopolymer mortar based on kaolinitic coal gangue," Case Studies in Construction Materials, vol. 18, pp. e01957, 2023.
[121]L. Vidal, E. Joussein, M. Colas, J. Absi, and S. Rossignol, "Effect of the addition of ammonium molybdate on metakaolin-based geopolymer formation: Shrinkage and crystallization," Powder Technology, vol. 275, pp. 211-219, 2015.
[122]M. F. Zawrah, S. E. A. Sawan, R. M. Khattab, and A. A. Abdel-Shafi, "Effect of nano sand on the properties of metakaolin-based geopolymer: Study on its low rate sintering," Construction and Building Materials, vol. 246, pp. 118486, 2020.
[123]A. Elimbi, H. K. Tchakoute, M. Kondoh, and J. D. Manga, "Thermal behavior and characteristics of fired geopolymers produced from local Cameroonian metakaolin," Ceramics International, vol. 40, no. 3, pp. 4515-4520, 2014.
[124]A. M. Rashad and A. S. Ouda, "Thermal resistance of alkali-activated metakaolin pastes containing nano-silica particles," Journal of Thermal Analysis and Calorimetry, vol. 136, no. 2, pp. 609-620, 2019.
[125]S. Yaşın and H. Ahlatcı, "Thermal investigation of fine alumina powder reinforced Na-metakaolin-based geopolymer binder for refractory applications," Journal of the Australian Ceramic Society, vol. 55, no. 2, pp. 587-593, 2019.
[126]E. Kamseu, A. Rizzuti, C. Leonelli, and D. Perera, "Enhanced thermal stability in K_2O-metakaolin-based geopolymer concretes by Al_2O_3 and SiO_2 fillers addition," Journal of Materials Science, vol. 45, no. 7, pp. 1715-1724, 2010.
[127]H. K. Tchakouté, C. H. Rüscher, S. Kong, E. Kamseu, and C. Leonelli, "Thermal behavior of metakaolin-based geopolymer cements using sodium waterglass from rice husk ash and waste glass as alternative activators," Waste and Biomass Valorization, vol. 8, no. 3, pp. 573-584, 2017.
[128]E. Kamseu, V. Catania, C. Djangang, V. M. Sglavo, and C. Leonelli, "Correlation between microstructural evolution and mechanical properties of α-quartz and alumina reinforced K-geopolymers during high temperature treatments," Advances in Applied Ceramics, vol. 111, no. 3, pp. 120-128, 2012.
[129]T. S. Lin, D. C. Jia, P. G. He, and M. R. Wang, "Thermo-mechanical and microstructural characterization of geopolymers with α-Al_2O_3 particle filler," International Journal of Thermophysics, vol. 30, no. 5, pp. 1568, 2009.
[130]E. Tiffo, J. B. B. Mbah, P. D. B. Belibi, J. N. Y. Djobo, and A. Elimbi, "Physical and mechanical properties of unheated and heated kaolin based-geopolymers with partial replacement of aluminium hydroxide," Materials Chemistry and Physics, vol. 239, pp. 122103, 2020.
[131]V. F. F. Barbosa and K. J. D. MacKenzie, "Thermal behaviour of inorganic geopolymers and composites derived from sodium polysialate," Materials Research Bulletin, vol. 38, no. 2, pp. 319-331, 2003.
[132]C. Nobouassia Bewa, H. K. Tchakouté, D. Fotio, C. H. Rüscher, E. Kamseu, and C. Leonelli, "Water resistance and thermal behavior of metakaolin-phosphate-based geopolymer cements," Journal of Asian Ceramic Societies, vol. 6, no. 3, pp. 271-283, 2018.